Proceedings of the
International Conference on Mechanical Engineering 2011
(ICME2011) 18-20 December 2011, Dhaka, Bangladesh

ICME11-KEY-02

EXPERIMENTAL TECHNIQUES FOR AEROACOUSTICS IN LOW MACH NUMBER CONFINED FLOWS

Hans Bodén, Sabry Allam Andreas Holmberg and Mats Åbom

KTH Linné Flow Centre, The Marcus Wallenberg Laboratory, SE-100 44 Stockholm, Sweden

ABSTRACT

Measurement of plane wave acoustic transmission properties, so called two-port data, of flow duct components is important in many applications such as in the development of mufflers for IC-engines. Measurement of two-port data is difficult when the flow velocity in the measurement duct is high because of the flow noise contamination of the measured pressure signals. The wall mounted pressure transducers normally used will pick up unwanted flow noise mainly in the form of turbulent pressure fluctuations. The problem is then obtaining a signal-to- noise ratio high enough for quality measurements. Techniques to improve acoustic two-port determination have been developed in this paper, including test rig design, signal processing techniques and over-determination.

Keywords: Duct Acoustics, Two-Port Measurements, Flow Noise Suppression, Wave Decomposition.

1. INTRODUCTION

The measurement of acoustic signals in the presence of masking noise, often generated by mean flow, is a ubiquitous problem in experimental flow duct acoustics. When performing acoustic tests in a flow duct facility, the researcher is faced with the task of obtaining a signal-to- noise ratio high enough for quality measurements. The signal-to-noise ratio is defined as the ratio of the sound power of the desired acoustic signal to the sound power of the (flow) noise. The ratio in dB is given by

$$SNR = 10 \log_{10}\left(\frac{P_S}{P_N}\right), \quad (1)$$

where P_S is the sound power of the acoustic signal and P_N is the unwanted noise sound power.

For measurements in flow ducts it is generally acknowledged that the transducers should be flush mounted in order not to give any extra disturbance to the noise or flow field. There are situations in which measurements have to be taken at different points over the duct cross sections see, e.g., [1]. This paper will however only consider flush mounted transducer configurations and measurement situations where the aim is to extract an acoustic signal coming from a machine or generated by loudspeakers from contaminating noise. Since the transducer surface is a flat surface while the duct might have a circular cross section perfect flush mounting might not be possible. Even if the transducers were perfectly flush mounted they would still pick up unwanted disturbances of two kinds. The first is incompressible turbulent pressure fluctuations or so called pseudo sound. The second is acoustic noise generated by the flow in the duct but propagating as acoustic waves. The pseudo sound is usually the dominating problem since the acoustic signal of interest, whether it comes from a machine or is generated by loudspeakers will usually be of higher level than the acoustic flow noise. One can try to shield the microphones from the flow noise in different ways using porous layers or slit tube microphones [1]. This can lead to calibration problems as well as to very long probes for low frequency measurements. In [2] small electret microphones coupled to the duct through a small hole and a cavity forming a Helmholtz resonator were used. In this paper a number of different microphone holder configurations were tested including one similar to the configuration suggested in [2].

It is possible to try to extract the acoustic signal from the contaminating noise by different signal processing techniques. A baseline method to compare the other techniques with is ordinary frequency domain averaging, the standard technique found in any FFT signal analyser [3-4]. It gives a reduction of stochastic fluctuation amplitudes [5,6] but it does not actually reduce the level of the flow noise and can therefore not be used to extract the acoustic signal when it is buried in the flow noise. Synchronised time domain averaging [7-15] on the other hand is a technique to extract a deterministic signal from additive noise. This technique requires a noise free reference signal for the synchronisation. Cross-spectrum based frequency domain averaging [16-20] is another candidate technique for extracting the acoustic signal. It requires a reference for which the unwanted noise is uncorrelated with the noise at the measurement transducer. It is not necessary that the signal is deterministic. Another technique for signal-to-noise ratio improvement, which has been proposed and tested with

reasonably good results, is the use of a hotwire probe and active control techniques in combination with the microphone [21-22]. The idea is that the hotwire probe mainly picks up the turbulent fluctuations which are then filtered our from the microphone signal using active control techniques. This method has not been tested in the present work due to the added complexity of introducing a hotwire probe and the problem of probe flush mounting.

There are several parameters that can be used to describe the acoustic performance of a duct element such as a muffler. These include the noise reduction (NR), the insertion loss (IL), and the transmission loss (TL). The transmission loss is the difference in sound power level between the incident and the transmitted sound wave when the muffler termination is anechoic. It is a property of the duct element under test only so it is helpful for instance in muffler design. In many cases the acoustic properties such as transmission and insertion losses can not be determined analytically, owing for instance to the complex geometry or the presence of the mean flow. Therefore experimental techniques must be used. The standard technique today for measuring acoustic plane wave properties in ducts, such as absorption coefficient, reflection coefficient and impedance is the two-microphone method (TMM) [24-36]. The sound pressure is decomposed into its incident and reflected waves and the input sound power may then be calculated. Many papers have been devoted to the analysis of the accuracy of the TMM for example [34-36].

Transmission loss can in principle be determined from measurement of the incident and transmitted power using the TMM on the upstream and downstream side of the test object provided that a fully anechoic termination can be implemented on the outlet side. It is however very difficult, to design an anechoic termination that is effective at low frequencies. An acoustical element, like a muffler, can also be modelled via its so-called four-pole parameters. Assuming plane wave propagation at the inlet and outlet, the four-pole method is a means to relate the pressure and velocity (particle, volume, or mass) at the inlet to that at the outlet. Using the four-pole parameters, the transmission loss of a muffler can also be readily calculated. Furthermore, if the source impedance is known, the four-pole parameters of the muffler can be used to predict the insertion loss of the muffler system.

The experimental determination of the four poles has been investigated by many researchers. To and Doige [37, 38] used a transient testing technique to measure the four-pole parameters. The technique was developed both for blockable, reciprocal systems and for non-blockable, non-reciprocal systems. This last case corresponds to cases with mean flow in the system. For such cases the technique requires pressure measurements (amplitude and phase) at four different duct cross sections, two before and two after the system under test. However, their results were not good especially at low frequencies. Lung and Doige [7] used a similar approach to measure the four-pole parameters of uniform tubes, flare tubes and expansion chambers, the presented experimental results until $M \approx 0.2$. Nishimura et al [39] have presented a method, which principally is equivalent to the method of Lung and Doige, using random excitation. Payri et al [40] developed a modified impulse method where weakly nonlinear transient effects could be taken into account. In references [37-39], the two different input states to the system were obtained by using a fixed acoustic source and two-different acoustic loads. The method can give large errors if the two loads are not "sufficiently" different over the entire frequency range.

Fumoux et al [41] describe a method to measure the transfer matrix of hydraulic piping system elements. In their method the test object is mounted in special rig terminated at each end by a source. The sources consisted of a piston driven by an electro-dynamic exciter. The matrix parameters were obtained by measuring the pressure and acceleration at the piston for two different source configurations. Doige and Munjal [43] have modified the method proposed in reference [38], The two different states are now obtained by changing the source location, with the rest of the system kept unchanged. As demonstrated in reference [43] the two-source method typically gives better results compared to the two-load method and it does not affect the mean flow field, since the geometry of the system is kept unchanged. Åbom [44] presented and tested a method for measuring the scattering-matrix, which is preferable to use since the scattering matrix gives the most basic description of the wave interaction problem. The scattering matrix describes the relation between the travelling wave amplitudes of the pressure on either side of the test object. The technique can easily be extended to the case of an arbitrary number of ports. A method to suppress disturbing flow noise was also described in [45], using a reference signal correlated with the acoustic field.

One aim of the present paper is to show how good two-port data measurements can be made for reasonably high flow velocities, up to M = 0.3. This requires that care is taken in designing the experimental setup and in choosing the signal processing techniques used. There have been previous articles published with similar subjects, as for instance [2], but the results presented were not very good at high flow velocities and the information given on how to perform the measurements was not very complete.

For linear, active multi-ports there are experimental methods with an external source and without an external source. The methods without an external source are so called multi-load methods [46] and are best suited when the source generated pressure amplitude is very high (> 130 dB in air). A typical example (one-port case) is the determination of acoustic source data on IC-engines [47-48]. If the source is of only moderate strength, the methods with external sources are preferable, since a better control of the sound spectrum and a better flow noise suppression is possible.

The methods with an external source are two-step methods. Firstly, the passive properties of the N-port and the reflections in the test rig are measured using an external source [49]. The main problem in the first step is to suppress flow noise and the two-port source itself. Secondly, the external source is shut off. For this measurement the flow noise in the test rig must be suppressed in order to resolve the sound generated by the

source under study. Terao and Sekine [50] presented the first paper describing the procedure to determine active two-port source data with application to axial fans. However, in their original work, the suggested flow ("turbulence") noise suppressing procedure only works when the acoustic fields on both sides of the two-port are completely coherent. Lavrentjev et al. [51] showed how this problem could be overcome by using one noise-free reference microphone on each side of the two-port. They also showed how a source vector with suppressed flow noise could be calculated directly from measured pressure cross spectra. The application studied in [51] was also an axial fan. The first demonstration that the measurement of active two-port data is also possible on weaker sources, i.e. flow generated in-duct sound at low Mach-numbers came with the paper by Allam et al. [52]. In that paper the procedure proposed by Lavrentjev et al. was successfully applied to determine the source data for an orifice plate (contraction ratio 0.28) for Mach-numbers (in the duct) up to 0.1. More recently, De Roeck and Desmet [53] again applied the method by Lavrentjev et al. to determine the flow generated sound by an expansion chamber muffler, and in a paper by Karlsson and Åbom [54] the method was applied for the source generation at a T-joint consisting of pipes with circular cross section.

Here, the method by Lavrentjev et al. [51] is extended into an over-determination method. This implies using microphones at more than 2 cross-sections on each side of the two-port to construct the estimate of the auto- and cross spectra of the source components. The improved method is applied to a determination of the broad band noise generated by a vortex mixer plate [74], and compared to the measured result of an empty duct representing the rig background noise. The reasons for the choice of application are two-fold – firstly, the sound generated is of a broad-band character, the studies of which are scarce in the literature. Secondly, the sound generated is of moderate strength, and it will be shown in the results that for some frequency bands the flow noise in the rig is of the same order of magnitude as the source generated sound. This requires measurements of high quality, representing a difficult measurement case for which the improvements in the methods can be tested vigorously. In order to obtain accurate propagation wave numbers, a method of refining the real part of the wave number, by numerically calculating the Mach number from the acoustic measurements, is introduced. To detect possible interactive effects between the acoustic and the hydrodynamic field, the power balance, as described in [54], is calculated from the measured scattering matrix.

Finally it should be noted that the theory and experimental setup presented in this paper can easily be extended to N-ports where N > 2.

2. FLOW NOISE SUPRESSION

The most common way of reducing wind noise is using a suitable windshield [55]. The effect of this type of device is most marked at velocities below 12 m/s. With higher flow rates the transducers will pick up the sum of the acoustic and turbulent pressure fluctuations. An efficient way of suppressing turbulent pressure fluctuations is to use a reference signal which is uncorrelated with the disturbing noise in the system and linearly related to the acoustic signal in the duct. A good choice for the reference signal is to use the electric signal driving the external sources as a reference. Deviation from a linear relation between the reference signal and the acoustic signal in the duct can for instance be caused by non-linearity in amplifiers and loudspeakers at high input amplitudes, temperature drift and non-linearity of the loudspeaker connections to the duct at high acoustic amplitudes. One possibility is to put an extra reference microphone close to a loudspeaker or even in the loudspeaker box behind the membrane, i.e., without contact with the flow. Otherwise one of the measurement microphones can be used as a reference. The disadvantage of this technique is that you will get a minimas at the reference microphone at certain frequencies or poor signal to noise ratio. To solve this problem you can use the microphone with the highest signal-to-noise ratio as the reference. This technique is tested in the present paper. A number of different signal processing techniques can also be used for reducing the effect of flow noise.

2.1 Frequency domain averaging (FDA)

The reference technique used in this study was ordinary frequency domain averaging which is the standard technique found in any FFT signal analyser. This method is sometimes known as the weighted, overlap, segment averaging (WOSA), Welch technique or Bartlett technique [3, 4]. The signal auto spectrum $G_{xx}(\omega)$ is measured and averaged according to,

$$\hat{G}_{xx}(\omega) = \frac{1}{N}\sum_{i=1}^{N} G_{xx}^{i}(\omega), \qquad (2)$$

where N is the number of averages. The variance of autospectral density estimates [5,6] is,

$$\sigma^2\left[\hat{G}_{xx}(\omega)\right] = \frac{G_{xx}^2(\omega)}{N}, \qquad (3)$$

which leads to the normalised random error,

$$\varepsilon_r\left[\hat{G}_{xx}(\omega)\right] = \frac{1}{\sqrt{N}}. \qquad (4)$$

This gives a reduction of stochastic fluctuation amplitudes by a factor $1/\sqrt{N}$. It does not actually reduce the level of the flow noise and can therefore not be used to extract the acoustic signal when it is buried in the flow noise.

2.2 Synchronised time domain averaging (STDA)

Synchronised time domain averaging [7-16] is a technique to extract deterministic signals which can be periodic or repeated transients, from additive noise. This technique requires a noise free reference signal for the synchronisation. It has been applied to analysis of sound and vibration of rotating machinery [12-14] where the reference signal can be a "tachometer" signal giving a number of pulses per revolution. A number of improvements to technique have been suggested [12-14]

to handle the effect of speed variations and other cycle-to-cycle variations. If the purpose of the measurement is system identification and the input signal is available as a reference or controlled from the signal analysis system this input signal can be used for the synchronisation. Examples of this type of measurements are modal analysis or determination of reflection and transmission properties of flow duct elements [7-9]. The time domain average is calculated by obtaining a number of synchronized time records of the signal *y(k)* with sample interval Δt. The signal is composed of the periodic, or repeatable transient, signal *x(k)* and the added noise signal *m(k)*,

$$y_i(k) = x(k) + m_i(k), \quad k = 0, 1, \ldots, K-1, \tag{5}$$

where *i* is the index of each time record and *K* is the number of samples for the time records. The estimate of *x(k)* from time domain average is then obtained by,

$$\hat{x}(k) = \frac{1}{N}\sum_{i=1}^{N} y_i(k). \tag{6}$$

where N is the number of averages. Since the periodic signal is synchronised in each time record while the noise is uncorrelated the noise signal will tend to cancel out. The signal-to-noise ratio will be improved by a factor *N*, or by $10 \cdot Log(N)$ dB [7,15]. In most cases the time averaged estimate of $\hat{x}(k)$ will be Fourier transformed to get the frequency spectrum in which case it is important that the acoustic signal is periodic in the time window used to avoid leakage effects.

2.3 Cross-spectrum based frequency domain averaging (CSFDA)

This technique can be used if a noise free reference is available. The reference signal can in fact be noisy as long as the unwanted noise in the reference signal and the measured noisy signal is uncorrelated. It is also not necessary that the signal is deterministic but in the present study we have used a periodic signal in the tests to make the results comparable to the results of synchronised time domain averaging. Cross-spectrum based techniques have for instance been used for intensity measurements using the signal driving the source as a reference [17] and in in-duct acoustic source characterisation [18]. The auto spectrum is estimated from,

$$\hat{G}_{xx}(\omega) = \frac{\hat{G}_{rx}^{*}(\omega)\hat{G}_{rx}(\omega)}{\hat{G}_{rr}(\omega)}, \tag{7}$$

where $\hat{G}_{xx}$ is the estimated auto-spectrum at the microphone position, $\hat{G}_{rr}$ is the auto-spectrum of the reference signal and $\hat{G}_{rx}$ is the cross-spectrum between the reference signal and the microphone signal. The reference signal can be the signal driving the source but it can also be another microphone signal providing that it is sufficiently flow noise free. The auto and cross spectrum estimates are obtained by averaging according to,

$$\hat{G}_{\gamma x}(\omega) = \frac{1}{N}\sum_{i=1}^{N} G_{\gamma x}^{i}(\omega), \tag{8}$$

where $G_{\gamma x}^{i}$ is the i:th auto or cross spectrum measurement and γ is *x* or *r*. The method relies on a linear relationship between the reference signal and the acoustic signal. If the signal driving the source, for instance the input signal to a power amplifier and a loudspeaker, is used as the reference this may not be fulfilled. When the flow noise level is high there is a natural tendency to raise the input level, which may make the relationship between the reference signal and the acoustic signal non-linear. The problem can be solved by using another microphone signal as the reference if a flow noise free mounting position can be found.

Another method for suppressing the flow noise using three microphones mounted in the duct was proposed by Chung and Blaser [19, 20]. This technique is based on the assumption that the disturbing noise signals at the three microphones are mutually uncorrelated. If two reference signals *r* and *q* are used, the expression for estimating the auto spectrum is,

$$\hat{G}_{xx}(\omega) = \frac{G_{qx}^{*}(\omega)G_{rx}(\omega)}{G_{rq}(\omega)}, \tag{9}$$

where $\hat{G}_{xx}$ is the estimated auto-spectrum at the microphone position, G_{qx} is the cross-spectrum between reference *q* and the microphone signal, G_{rx} is the cross-spectrum between reference *r* and the microphone signal and G_{rq} is the cross-spectrum between the two reference signals. Since only cross spectras are used it is not required that the reference signals are completely noise free. It is sufficient that the additive (flow) noise signals at the reference positions and at the measurement position are mutually uncorrelated.

If the acoustic signal is deterministic and a noise free reference signal is available it is possible to average the Fourier spectra directly. By taking the Fourier transform of both sides of equation

(6) we get,

$$\hat{X}(\omega) = \frac{1}{N}\sum_{i=1}^{N} Y_i(\omega), \tag{10}$$

where $\hat{X}(\omega)$ is the estimated Fourier spectrum at the microphone position and $Y_i(\omega)$ is the i:th Fourier spectrum of the microphone signal. It can be expected that the flow noise suppression in

(10) will be the same as for

(6) that is, a signal-to-noise ratio improvement by a factor *N*, or by $10 \cdot Log(N)$ dB.

The normalised random errors in the cross spectra estimates in

(8) can according to [6] be given by,

$$\varepsilon_r\left[\hat{G}_{ry}(\omega)\right] = \frac{1}{\left|\gamma_{ry}^{2}(\omega)\right|\sqrt{N}}, \tag{11}$$

where $\gamma_{ry}^2(\omega)$ is the coherence function between the reference and the microphone signal. This means that the signal-to-noise ratio also when performing the averaging according to
(8) can be expected to improvement by a factor *N*, or by $10 \cdot Log(N)$ dB.

3. EXPERIMENTAL TECHNIQUES AND TEST SET-UP

3.1 Experimental Characterization Of Two-Ports

For a linear acoustic duct element with one input and one output end, and where both sides are acoustically coupled, the model best suited is the two-port model [56]. There exist several different formulations of a two-port [56-58]. However, each can be obtained from a linear transformation of the others. If the state variables chosen are the acoustic pressure (*p*) and volume velocity (*q*), depending on the choice of input and output state vectors the model is either referred to as a mobility matrix [56] or as a transfer matrix model [57]. Davies [58] introduced a variant referred to as the two-port scattering matrix model, in which the pressure wave amplitudes on both sides are directly related. Åbom [59] argued that the scattering matrix formulation is preferable over the transfer matrix since it best describes a wave-interaction problem. The scattering matrix (**S**) formulation of a two-port can in the frequency domain be written as

$$\underbrace{\begin{bmatrix} p_{a+} \\ p_{b+} \end{bmatrix}}_{p_+} = \underbrace{\begin{bmatrix} \rho_a & \tau_{ba} \\ \tau_{ab} & \rho_b \end{bmatrix}}_{S} \underbrace{\begin{bmatrix} p_{a-} \\ p_{b-} \end{bmatrix}}_{p_-} + \underbrace{\begin{bmatrix} p_{a+}^s \\ p_{b+}^s \end{bmatrix}}_{p_+^s} \tag{12}$$

where *a* and *b* refers to the two sides of the two-port, the plus and minus signs indicate propagation outwards and into the two-port respectively, the superscript *s* refers to source generated sound, and ρ describes the reflection and τ the transmission of incoming waves. The definition of propagation directions and other indices are shown in Fig. 1. Throughout this paper, an exp(iωt) time dependence is assumed.

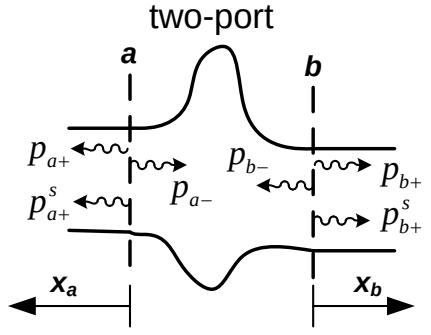

Figure 1 Schematic of a two-port illustrating the convention for positive directions used in this paper.

3.2 Wave Decomposition Methods

As stated in the introduction, the experimental determination of a two-port model is based upon methods to decompose the sound field into waves propagating in the downstream and upstream directions. The two microphone wave decomposition method was first introduced by Schmidt and Johnston [60]. They showed how the acoustic reflection of a test sample in a duct with a mean flow could be obtained from measurements, using a loudspeaker with stepped sine excitation, and by having two microphones a distance apart to decompose the field into opposite propagating waves. Seybert and Ross [27] extended the method to work with broad band excitation, and they also described why the method fails when the intermediate distance between the microphones equals half an acoustical wavelength. This problem can be avoided by having multiple microphones covering the complete frequency range of interest. Multiple microphones also enables an extension of the two microphone method into an over-determined system of equations [61, 62], or into a non-linear equation system with both the complex wave numbers and pressure amplitudes as unknowns [64].

3.2.1 The two-microphone method

All wave decomposition methods mentioned above are based on the following equation relating acoustic pressure to propagating wave amplitudes, referred to as the two-microphone method:

$$\underbrace{\begin{bmatrix} e^{-ik_+x_1} & e^{ik_-x_1} \\ e^{-ik_+x_2} & e^{ik_-x_2} \end{bmatrix}}_{A} \underbrace{\begin{bmatrix} p_+ \\ p_- \end{bmatrix}}_{p_\pm} = \underbrace{\begin{bmatrix} p_1 \\ p_2 \end{bmatrix}}_{p} \tag{13}$$

where $k_\pm$ are the wave numbers for planar waves. Neglecting losses these wave numbers are given by

$$k_\pm = \frac{\omega}{c_0} \frac{1}{1 \pm M} \tag{14}$$

where *M* is the mean Mach number, ω is the angular frequency and c_0 is the ambient speed of sound. In this paper, due to the fact that the positive axis is directed towards the flow on the upstream side, the sign in front of the Mach number in Eq. (14) must be changed for waves on the upstream side. For the system in Eq. (13) to be solvable, the two equations must be linearly independent, i.e. the determinant of **A** must be non-zero [34, 35]. This implies a criterion on the Helmholtz number, based upon the separation between pressure sampling points x_1 and x_2,

$$(x_2 - x_1)(k_+ + k_-) \neq 2n\pi, \qquad n = 1,2 \ldots \tag{15}$$

which, using the wave numbers from Eq. (14) can be written as

$$\frac{\omega}{c_0}\frac{(x_2 - x_1)}{1 - M^2} \pm n\pi \tag{16}$$

However, even though the two microphone method in theory works when Eq. (16) is satisfied, the method is very sensitive to errors when the microphone distance is close to half a wavelength. In order to take various types of errors into account, Åbom and Bodén [35] suggested that the criterion should be altered

$$0.1\pi < \frac{\omega}{c_0}\frac{(x_2 - x_1)}{1 - M^2} < 0.8\pi \tag{17}$$

They also pointed out that the total error from all disturbances will be smallest in a region around

$$\frac{\omega}{c_0}\frac{(x_2 - x_1)}{1 - M^2} = \frac{\pi}{2} \tag{18}$$

By sampling the field at more than two positions along the duct it is possible to broaden the frequency band in which the error sensitivity is kept low. Here methods of utilizing an array of $n > 2$ positions (microphones) will be discussed. For the two-microphone method, it is obvious that for a given frequency, the microphones used should be the pair with the intermediate distance that best fulfills Eq. (18). Thus, an optimum array for this method would consist of gradually increasing distances between each microphone pair. However, the optimum microphone array differs between the methods. One aim of this paper is to evaluate the applicability of the methods for the array used in the source determination.

3.2.2 *The wave decomposition over-determination method*

For a set of n microphone positions we can define a function $\boldsymbol{f}$ as

$$f_j = p_+ e^{-ik_+ x_j} + p_- e^{ik_- x_j} - p_j \tag{19}$$

Fujimori et al [61] formulated the problem as a least squares problem in which the Euclidian norm of $\boldsymbol{f}$ is to be minimized, a problem equivalent to solving the over-determined system

$$\underbrace{\begin{bmatrix} e^{-ik_+ x_1} & e^{ik_- x_1} \\ e^{-ik_+ x_2} & e^{ik_- x_1} \\ \vdots & \vdots \\ e^{-ik_+ x_j} & e^{ik_- x_1} \end{bmatrix}}_{A} \underbrace{\begin{bmatrix} p_+ \\ p_- \end{bmatrix}}_{p_\pm} = \underbrace{\begin{bmatrix} p_1 \\ p_2 \\ \vdots \\ p_j \end{bmatrix}}_{p} \tag{20}$$

which is solved by the Moore-Penrose pseudo-inverse [63]. Just as before, the system will be solvable when at least two rows in **A** are linearly independent. Here there are two possibilities, either all microphones are put into the equation system or, when possible the over-determination is used with a set of microphones in which all intermediate distances satisfy Eq. (17). Of all such sets, it is appropriate to select the one with the largest number of microphones. Jang and Ih [48] concluded in their work that an equidistant microphone spacing yields the most accurate results for this over-determination method.

3.2.3 *The multi-point method*

Parrott and Jones [62] applied the method of weighted residuals in order to minimize $\boldsymbol{f}$ in Eq. (19). For an array with n microphones they setup the two equations

$$\sum_{j=1}^{n} \left(p_j - p_+ e^{-ik_+ x_j} - p_- e^{ik_- x_j}\right) e^{-ik_+ x_j} = 0 \tag{21}$$

and

$$\sum_{j=1}^{n} \left(p_j - p_+ e^{-ik_+ x_j} - p_- e^{ik_- x_j}\right) e^{ik_- x_j} = 0 \tag{22}$$

which can be solved analytically if the wave numbers are known. In their work they tested up to six microphone positions per half a wavelength, using three different arrays of microphones. They also concluded that arrays with equidistant microphone spacing yield the best results, and that their method is superior to the two microphone method if more than two microphone positions are used.

3.2.4 *The full wave decomposition method*

When the number of microphones is at least four, it is possible to use the full wave decomposition method described by Allam and Åbom [64], in which both the complex pressure amplitudes and the complex wave numbers are solved for. This is done by applying a damped Gauss-Newton algorithm [63] on Eq. (21). In order to setup the iteration process, initial values of the variables must be obtained. The wave numbers can be obtained from a model proposed by Dokumaci [65] which includes the effects of visco-thermal damping

$$k_\pm = \frac{\omega}{c_0}\frac{K_0}{1 \pm K_0 M} \tag{23}$$

where K_0 is given by

$$K_0 = 1 + \left(\frac{1-i}{s\sqrt{2}}\right)\left(1 + \frac{\gamma - 1}{\sqrt{Pr}}\right) \quad (24)$$

where $s = r\sqrt{\rho_0 \omega / \mu}$ is the shear wavenumber, μ is the dynamic viscosity, r is the duct radius, ρ_0 is the ambient density, γ is the ratio of the specific heats and Pr is the Prandtl number. The initial values of the pressure amplitudes are then found by using the initial values of the wave numbers and Eq. (13). In their work, Allam and Åbom [64] successfully obtained the complex wave numbers using two separate (~3 m) clusters of microphones. The imaginary part corresponds to the acoustic attenuation as the wave propagates and, compared to the real part, it has a small influence except for large Helmholtz-numbers (based on the propagation distance). Thus it is not always required or possible to obtain the imaginary part experimentally. For the real part, the main error in the wave number model stems from the determination of the mean Mach number. A traditional way of obtaining the mean flow velocity is by measuring the maximum velocity in the duct using a Prandtl pipe, then assuming a fully developed turbulent flow and applying a suitable velocity power law profile, e.g. 1/7 see Ref. [66], which yields the correction factor between the maximum and mean flow speeds. The error is then due to measurement errors and deviations from the empiric power law, i.e. due to deviations between the assumed and the actual flow velocity profile. Such deviations are a problem in practice since the long undisturbed straight duct section (> say 50 duct diameters) required for a fully developed turbulent profile can be difficult to realize. For an array with two widely separated microphone clusters there are methods to obtain the mean Mach number from plane wave acoustic measurements, e.g. see Ref. [67-69].

3.2.5 Mach number determined from the full wave decomposition method

Here another approach of obtaining the real part of the wavenumbers, based upon the solution of the non-linear equation system (21) is presented. Firstly, for each frequency point, the initial values of the wave numbers are determined using Eq. (21) and an adequate initial guess of the mean Mach number, e.g. based on a measurement. After the initial complex pressure amplitudes are determined, the system is solved for using the Gauss-Newton algorithm. Then, for each frequency point, the mean Mach number is determined from the real part of Eq. (21), and the result is averaged over the frequency range. The process is then repeated using the new Mach number for the calculations of the initial wavenumbers. When the Mach number has converged the iteration is stopped and the improved mean Mach number estimate can be put into Eq. (23) in order to get a more accurate wavenumber for the wave decomposition methods.

3.3 Measurement Of The Scattering Matrix

The scattering matrix contains four parameters and thus in order to obtain it, four equations are needed, in which all other quantities are known. Considering the wave decomposition methods discussed earlier, it is apparent that two of these equations are obtained from a measurement of the sound field on both sides of the two-port. The other two equations can be obtained by modifying the sound field and perform a second measurement.

The methods of modifying the sound fields can basically be described as variants of any of the two measurement categories with an external source and without an external source. A review of the available methods can be found in [46]. The advantage of using an external source is that a better control of the sound spectrum is possible, but the drawback is that it may be impossible to use the method when the source sound level of the two-port becomes high. Here, were flow generated sound at moderate Mach-numbers is investigated, this is not a problem, and, therefore, methods with an external source is preferred. The different sound fields can then be obtained by either changing the acoustic load of the system [46-48], or by changing the location of the excitation, as described by Munjal and Doige [49]. The latter approach is preferred, since by changing the load the pressure loss in the test rig may change, which can alter the volume flow through the system. In this work, a set of wall mounted loudspeakers covered with perforated plates at the opening to minimize any flow disturbance (see Fig. 2) are utilized to produce a stationary sound field in the test rig.

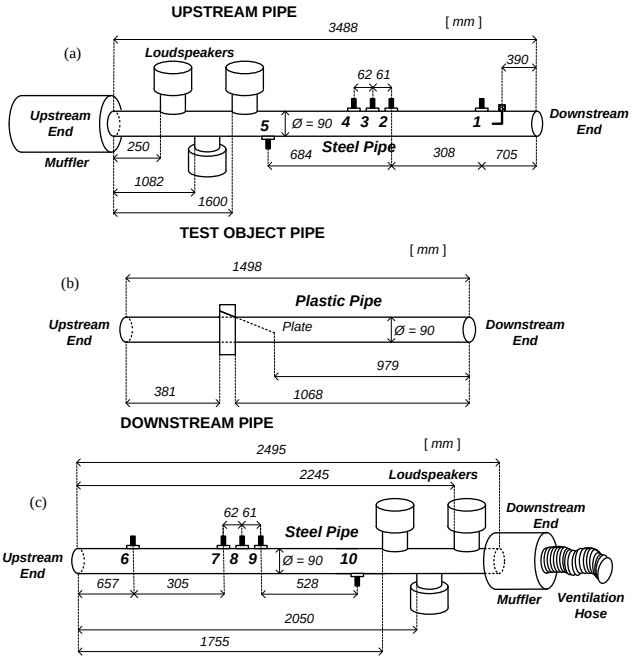

Figure 2 Test rig used in the experiments, (a) upstream pipe with Prandtl tube for flow speed data, (b) test object pipe, (c) downstream pipe. **1-10,** microphone positions.

Using different phase combinations of the loudspeaker signals, it is possible to create several independent test (load) cases for the two-port. Denoting the pressure amplitudes obtained in this manner by $N = I$,

II... we can write

$$\underbrace{\begin{bmatrix} p_+^I & p_+^{II} & \cdots & p_+^N \end{bmatrix}}_{P_+} = \underbrace{\begin{bmatrix} \rho_a & \tau_{ba} \\ \tau_{ab} & \rho_b \end{bmatrix}}_{S} \underbrace{\begin{bmatrix} p_-^I & p_-^{II} & \cdots & p_-^N \end{bmatrix}}_{P_-} \tag{25}$$

which is solved by

$$\boldsymbol{S = P_+ P_-^{-1}} \tag{26}$$

where the matrix inversion should be interpreted as a Moore-Penrose pseudo-inversion if the matrix is not square. The idea of this over-determination was first suggested by Åbom [55], and tested by Allam et al [70] for an orifice at $M < 0.1$, demonstrating that the results could be significantly improved using five different loudspeaker combinations. As previously discussed, in order for Eq. (25) to be valid, it is required that at least two among the pressure amplitude vector sets are linearly independent. If more than two are available all may be used. However, another approach is to discard some of the measurements based upon the coherence function.

It should be noted that for any of the methods described above to work when there is a mean flow present, a method to suppress the local flow turbulence noise should be applied. If an external signal correlated with the sound waves emitted by (all) the loudspeakers exists, e.g. the input voltage, uncorrelated signal content will be suppressed when the cross spectrum between the input signal and a microphone signal is averaged [45]. In this paper the index convention used for the cross spectra is

$$G_{ab} = a^* b \tag{27}$$

where the superscript * denotes complex conjugation. The cross spectrum is used together with the auto spectrum of the input signal (loudspeaker voltage *e*) to form an estimation of a transfer function

$$H_{ep} = {G_{ep}}/{G_{ee}} \tag{28}$$

This transfer function is then used in place of the microphone pressure signals in all the equations involving external source (loudspeaker) excitation.

3.4 Measurement Of The Source Strength

The main challenge in measuring the source of a two-port is to distinguish the sound generated by the element from other sound sources that may exist in the measurement rig. In addition, local turbulence will reduce the signal to noise ratio. Unlike for the measurements of **S**, this problem cannot generally be redeemed by using a reference signal when measuring on flow generated noise sources, although there are sources, e.g. fluid machines, for which a signal correlated with the tonal part of the generated sound exist. Also, the contribution from reflections and transmissions in the test rig must be taken into account, which means that both the scattering matrix of the two-port element and the passive properties of the test rig itself must be known. The latter are represented by reflection coefficients, which for a (passive) duct end termination (say) a can be written as

$$R_a = \frac{p_{a-}}{p_{a+}} \tag{29}$$

Any sound emitted in the test rig beyond the cross section of the reflection coefficient – be it flow noise or sound from a loudspeaker – will result in errors in this formula and must be suppressed. Therefore the loudspeakers on the side where the reflection coefficient is to be determined must be switched off for that measurement.

3.4.1 The source cross spectrum matrix

Once the reflection coefficients and the scattering matrix are known, the source vector can be equated as a function of the microphone pressure $\boldsymbol{p}$ (with loudspeakers switched off) at the reference cross section on each side of the two-port via [18]

$$\boldsymbol{p_+^s = (E - SR)(E + R)^{-1} p = Cp} \tag{30}$$

where $\boldsymbol{E}$ is the identity matrix and with

$$\boldsymbol{R} = \begin{bmatrix} R_a & \mathbf{0} \\ \mathbf{0} & R_b \end{bmatrix} \tag{31}$$

For random signals the source vector formulation is inadequate, and a more general description of the source is the source cross spectrum matrix

$$\boldsymbol{G^s = p_+^s (p_+^s)^H} = \begin{bmatrix} G_{p_{a+}p_{a+}} & G_{p_{b+}p_{a+}} \\ G_{p_{a+}p_{b+}} & G_{p_{b+}p_{b+}} \end{bmatrix} \tag{32}$$

where G_{ab} is the single sided spectrum of the signals *a* and *b*, and the superscript ^{H} refers to a complex conjugated and transposed quantity, i.e. the Hermitian transpose. The diagonal elements of the source cross spectrum matrix represent the auto spectra of the two source components, which are crucial in determining the sound power of the source. However, also of interest are the cross diagonal elements, i.e. the estimated cross spectra between the source components. Since they also

contain phase information they are more difficult to obtain. However in principle they will together with the auto spectra enable calculation of the coherence function between the source components [18], which can be used to describe the compactness of the source. A value of unity indicates that there is only one source present, while a lower value should be interpreted as a distribution of sources

Since Eq. (32) contains auto spectra, uncorrelated sound will still influence the results. Lavrentjev et al. [18] suggested using microphones at two different cross sections at each side to estimate the source data. The method is based upon the fact that if the distance between two microphones is long enough, the turbulent flow noise will be uncorrelated. This distance can, using the model of Corcos, be estimated from [35]

$$\Delta x > \frac{U}{f} \tag{33}$$

In order to combine the data at two different cross-sections transformation equations are required. The transformation of the scattering and the reflection matrix from the reference section to a new (primed) section is given by

$$S' = T_+ S T_-^{-1}, \qquad R' = T_+^{-1} R T_- \tag{34, 35}$$

where

$$T_+(x') = \begin{bmatrix} e^{-ik_{a+}x'_a} & 0 \\ 0 & e^{-ik_{b+}x'_b} \end{bmatrix}, \quad T_-(x') = \begin{bmatrix} e^{ik_{a-}x'_a} & 0 \\ 0 & e^{ik_{b-}x'_b} \end{bmatrix} \tag{36}$$

A transformed source vector can then be defined using the primed quantities above, and then transformed back to the original cross section, via

$$p_+^s = T_+^{-1}(x') p'^s_+, \tag{37}$$

which can be rewritten using Eq. (30)

$$p_+^s = T_+^{-1}(x')(E - S'R')(E + R')^{-1} p' \tag{38}$$

Introducing $C' = T_+^{-1}(x')(E - S'R')(E + R')^{-1}$, the source cross spectrum matrix can be written as [18]

$$\mathbf{G}^s = \mathbf{p}_+^s \left(\mathbf{p}_+^s\right)^\dagger = \mathbf{C} \begin{bmatrix} G_{p_a p'_a} & G_{p'_b p_a} \\ G_{p'_a p_b} & G_{p_b p'_b} \end{bmatrix} \mathbf{C}'^\dagger \tag{39}$$

Here only cross spectra are used, and thus uncorrelated contributions to the spectra will be suppressed.

3.4.2 Over-determination method

It has already been shown that we can write a source vector at the origin, defined as a function of the microphone pressure at a cross section *n*, via

$$p_+^s = C_n p_n \tag{40}$$

where

$$C_n = T_+^{-1}(x_n)(E - S_n R_n)(E + R) \tag{41}$$

Now, by rearranging this we get

$$C_n^{-1} p_+^s = p_n \tag{42}$$

If $n > 2$ microphones are available on each side of the two-port, one can use a subset of this, say n', to determine the source vector. If $n'>2$ this results in an over-determination which using Eq. (42) can be written as

$$\begin{bmatrix} C_1^{-1} \\ C_2^{-1} \\ \vdots \\ C_{n'}^{-1} \end{bmatrix} p_+^s = \begin{bmatrix} p_1 \\ p_1 \\ \vdots \\ p_{n'} \end{bmatrix} \tag{43}$$

This equation is best solved by the Moore-Penrose inversion algorithm. Now, assuming we divide the original set n into two-subsets with m' and n' microphones, respectively, where $m' + n' = n$ and m', $n' > 2$, then it is possible to over-determine two source pressure vectors by applying Eq. (43) to each set. It is then possible to write equation Eq. (39) as

$$G^s = \begin{bmatrix} C_1^{-1} \\ C_2^{-1} \\ \vdots \\ C_{m'}^{-1} \end{bmatrix}^{-1|} G \begin{bmatrix} C_1^{-1} \\ C_2^{-1} \\ \vdots \\ C_{n'}^{-1} \end{bmatrix}^{-1|} \tag{44}$$

where **G** is a $2m'$ x $2n'$ matrix with elements $G_{ij} = G_{p_j p_{i'}} \qquad i = 1,2 \ldots 2m', \qquad j = 1,2 \ldots n'$.

Thus, the four elements in $\mathbf{G}^s$ are now calculated from $2m'$ x $2n'$ cross spectra, which all should be formed from

microphone pairs satisfying Eq. (33). A given set of microphones will allow for several different calculations of the source vector. It can be noted though, that cross spectra are not formed using two signals from the same microphone pressure vector. For the purpose of optimizing the number of elements in **G** this implies that microphones mounted close to each other, i.e. not satisfying Eq. (33), should be put in the same microphone subset. Also, for this purpose the number of microphones used for each of the two source pressure vectors should be as equal as possible, since $m'n' \leq \left({}^{n}/_{2}\right)^{2}$. In order to setup guidelines for the range of applications and parameter values (e.g. Mach number and signal to noise ratio) for which the over-determination method will give an improvement, it is interesting to investigate the influence of various types of input errors, e.g. erroneous scattering matrix elements, local flow noise errors and external sound source contributions (bias errors). A first attempt towards these guidelines have recently been conducted [40], where it was found that the over-determination method was just as stable as the original method, and in addition managed to improve the results for input errors in the reflection coefficients and in the microphone data during the source measurement (when the loudspeakers are switched off).

2.4 Measuring Fluid-Acoustic Interaction Effects

If interaction occurs between the hydrodynamic and the acoustic fields, attenuation and amplification of the acoustic field can result. Since the interaction in the linear regime is triggered by acoustic waves, the process is correlated by the incident field. Thus, correlation techniques will not suppress any contribution due to this, and the resulting scattering matrix will hence describe attenuation and amplification in addition to reflection and transmission. A complete study of an aero-acoustic two-port should, therefore, in general include the interactive effects. The amount of amplification and attenuation of an incident wave spectrum can be described by a power balance [54], in which all test rig terminations are assumed anechoic. The power balance is defined as

$$\langle W_{rel} \rangle = {\langle W_{out} \rangle}/{\langle W_{in} \rangle} \tag{45}$$

where *W* refers to the acoustic power, and the subscript *rel* refers to the relative ratio of outgoing over incoming acoustic power. The power balance for incident power on the upstream side *a* is for constant density, cross sectional area and speed of sound over the two-port given by

$$\langle W_{rel} \rangle^{a} = \frac{|\rho_a|^2(1-M_a)^2}{(1+M_a)^2} + \frac{|\tau_{ab}|^2(1+M_b)^2}{(1+M_a)^2} \tag{46}$$

For sound power incident on the downstream side *b*, the power balance is instead

$$\langle W_{rel} \rangle^{b} = \frac{|\rho_b|^2(1+M_b)^2}{(1-M_b)^2} + \frac{|\tau_{ba}|^2(1-M_a)^2}{(1-M_b)^2} \tag{47}$$

The ratios will be larger than unity for amplification and smaller than unity for attenuation of the incident power. This analysis is similar to a more generic approach suggested by Aurégan and Starobinski [71], and is also sometimes referred to as the whistling potentiality. This is because a resonance in the rig, which coincides in frequency with an amplification region in the power balance, can lead to a whistle. Whether an actual whistling will occur can be determined by considering a Nyquist plot of the function [72]

$$D = det(\boldsymbol{E} - \boldsymbol{SR}) \tag{48}$$

Where **R** and **E** are defined as in Eqs. (20-31). If the function **D** encircles the origin in the Nyquist plot, the system is unstable at the corresponding frequency and a whistling will occur. Karlsson [72] showed in his experiments that using this analysis method it is possible to predict the reflections necessary for obtaining a whistle, and at which frequency it will occur. Kierkegaard and Efraimsson [73] recently applied the method on a scattering matrix of an orifice plate, obtained from linear CAA simulations, and were able to experimentally validate the predicted whistling conditions. This shows one of the main features of the scattering matrix formulation; as soon as the scattering matrix is known, it can be used to predict scattering and whistling for arbitrary while still linear end terminations.

3.5 Test Setup for signal-to-noise ratio enhancement tests

Experiments were carried out at ambient temperature using the flow acoustic test facility at The Marcus Wallenberg Laboratory for sound and vibration research KTH [23]. The test ducts used during the experiments on the effect of test rig configuration and signal processing techniques on the flow noise suppression consisted of standard steel-pipes with a wall thickness of 3 mm. The duct diameters were chosen to fit the test objects. Eight loudspeakers were used as acoustic sources, as shown in Fig. 3. The loudspeakers were divided equally between the upstream and downstream side. Each loudspeaker was mounted in a short side-branch connected to the main duct. The distances between the loudspeakers were chosen to avoid any minima at the source position. Fluctuating pressures were measured by using six condenser microphones (B&K 4938) flush mounted in the duct wall. The measurements were carried out using different types of signals, swept-sine, saw tooth and random noise and with different number of averages in time and frequency domain. The two-port data was

obtained using the source switching technique as described in reference [44]. The flow velocity was measured using a pitot-tube and a hot wire anemometer connected to an electronic manometer (Swema Air 300). It was measured at a distance ten times the duct diameters from the loudspeakers and six times the duct diameters from the test object diameter in order to avoid any flow disturbance. The flow upstream and downstream of the test object was measured separately before and after the acoustic measurements and the average result was used. The transfer functions between the reference signal and the microphone signals was measured and used to estimate the scattering matrix components.

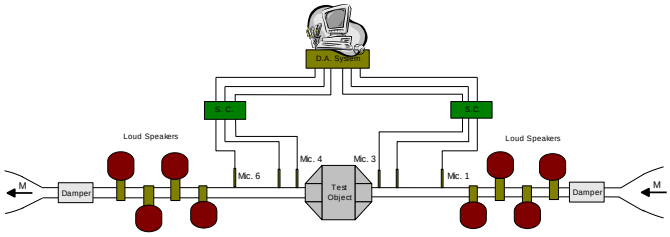

Fig 3. Layout of the test object

The test rig for determination of active and passive two port properties is shown in Fig. 2 and uses the same type of equipment,

3.5.2 Microphone calibration

The fluctuating pressures measured at each position have been corrected using the relative calibration between the microphones channels. Assuming that we have plane waves in a duct the sound pressure amplitude will be constant over the duct cross-section. If now the measurement microphones are placed at a duct cross-section and the sound pressure is measured all microphones would give the same pressure amplitude with zero phase shifts. However there will in practice be a deviation from this ideal case due to the measuring chain, amplifiers, cables etc., which introduce amplitude and phase shifts. Relative calibration of the microphone measurement chain is therefore needed. In order to calculate the scattering-matrix equation, the transfer function between the microphones and the electrical loudspeaker signal, i.e. H_{r1}, H_{r2}, H_{r3}, H_{r4}, H_{r5}, and H_{r6} are needed. It is sufficient to measure the transfer function between a reference microphone say microphone 1 and the other microphones, H_{12}, H_{13}, H_{14}, H_{15}, and H_{16}. A special calibration tube as shown in 4, has been built in order to measure the transfer functions between the reference microphone and the other microphones. The calibration tube consists of a loudspeaker, a steel pipe, which has the same diameter as the test object and a microphone holder for six microphones. The holder was made of a plastic material to avoid possible grounding errors between the microphones. The length of the steel pipe is preferably short to minimize the number of resonances in the pipe.

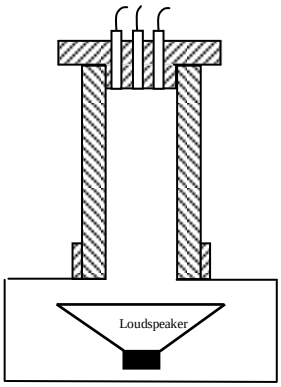

Fig 4. calibration tube.

3.5.3 Microphone holder configurations tested

The effect of a number of microphone holder configurations on the signal-to-noise ration has been studied. Six different holders, as shown below, were tested for different flow Mach numbers from 0.07 to 0.26. The test cases were:

1. The reference holder is shown in 5. The hub of the holder can be changed with the microphone diameter and the pipe dimension to fix the microphone flush with the pipe wall.
2. The microphone was connected to the measurement pipe through a 1 mm diameter hole in the pipe wall as shown in 6. The idea is to avoid flow separation just as in [2].
3. The same as 1 but with the microphone moved 1.5 mm up into the hub, forming a small cavity in front of the microphone. The resonance frequency of the quarter wave resonator formed by the cavity is 57 kHz.
4. The same as 3 but with the microphone moved 3 mm up into the hub. The resonance frequency of the quarter wave resonator formed by the cavity is 28 kHz.
5. The microphone was connected to the measurement pipe through a 30 mm long and 2 mm wide axial slit in the pipe.
6. A 6.4 mm diameter hole was added to the slit of holder 5 for fixing the microphone flush to the pipe wall.

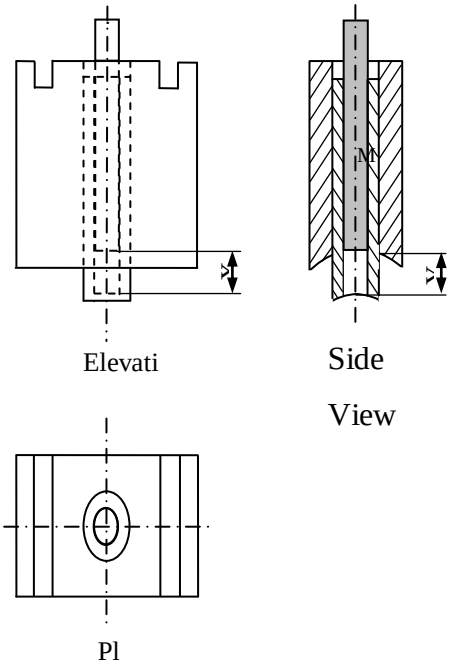

Fig 5. Construction drawing for the reference holder. X=0 for flush mounting. For holder configurations 3 and 4 the microphone was moved up into the hub, X =1.5 mm for holder 3 and X =3 mm for holder 4. Y can be changed according to the pipe wall thickness.

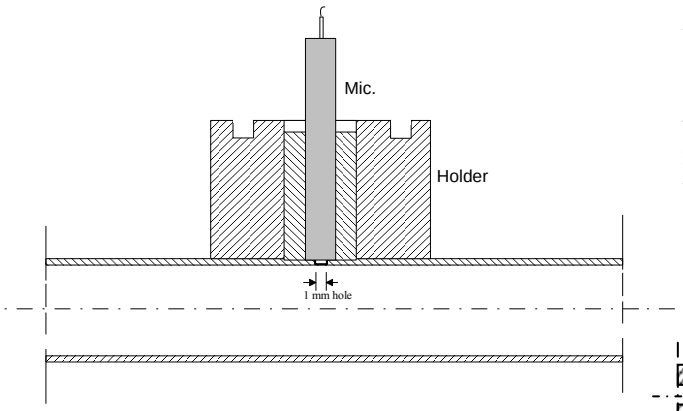

Fig 6. Cross section of the holder used for configuration 2.

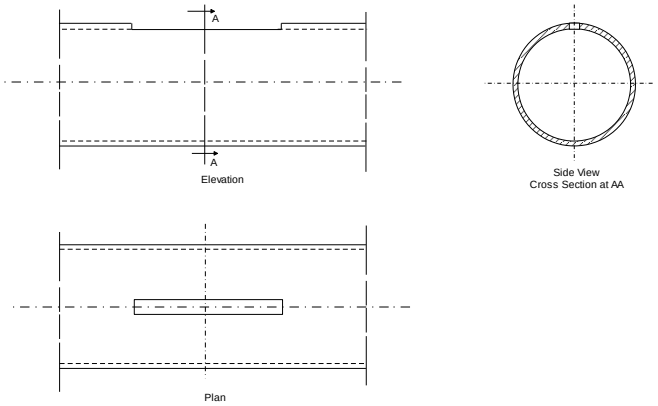

Fig 7. Slit in the pipe used for holder configuration 5.

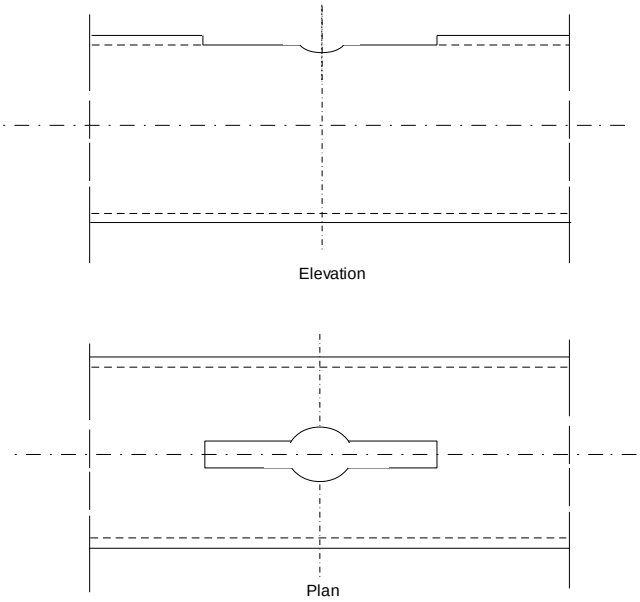

Fig 8 Slit (30 x 2) and ∅ 6.4 mm hole used for holder configuration 6.

3.5.4 Loudspeaker connections tested

Different configurations of loudspeaker connections to the duct, shown in Figure 9, have been studied at different Mach numbers from M=0.15 to M=0.3. For each loudspeaker configuration the signal-to-noise ratio was measured at all six microphone positions. This was made both with the source upstream and downstream of the test object.

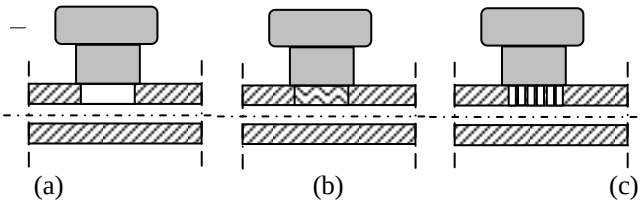

Fig 9 Loudspeaker connection configurations tested: a) loudspeaker connected using an open hole, b) as a) but with the hole filled with absorbing material, c) loudspeaker connected using a perforate pipe with 50% porosity.

3.5.5 Test objects

For this study three test objects have been chosen. A straight hard-walled duct with 47 mm inner diameter and 1000 mm length for which the acoustic two ports is known theoretically. An expansion chamber which can be seen in Fig. 10, with dimensions listed in Table 1. A commercial muffler is shown in Figure 11. The theoretical prediction of acoustic transmission properties for such a muffler is difficult and the muffler gives very high transmission loss which makes the measurements

difficult even without flow.

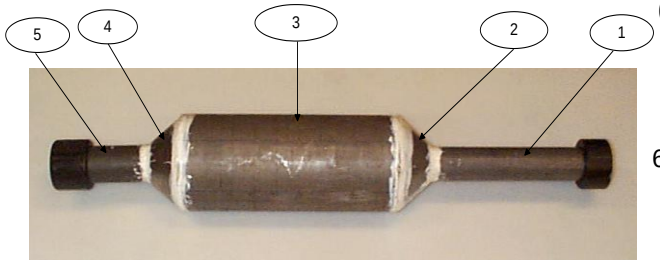

Fig 10. Picture for the expansion used in the experiments.

Table 1: Dimension of the expansion chamber components

Element number	Length×10^2 m	Diameter ×10^3 m
1	50	52
2	6.6	51/149
3	41	149
4	7.1	149/60
5	20	60

.

Fig 11. Picture for the commercial muffler used in the experiments.

The acoustic two-ports for tall three test objects have been measured using three different types of signals: random noise, stepped sine and saw-tooth excitation. The saw-tooth excitation was chosen to be able to perform synchronous time domain averaging (STDA). The comparison have been made for different flow speeds up to M= 0.32.

To test the source determination methods, they are applied on flow generated sound of a broad band character, produced at Mach 0.2 by a vortex mixer [74] in the form of a triangular plate, see Fig. 12. The plane wave decomposition methods are evaluated by measuring the scattering matrix of the plastic pipe with the plate mounting without the triangular plate in place. The results of such a measurement can help deducing which effects are due to the plate, and which are due to the rest of the test rig. The reason for the choice of plastic material in the test rig is to enable for optical access (e.g. PIV) in another project. Additionally, the author's believe the acoustic properties of the plastic pipe to be of interest to researchers planning to perform duct acoustics, in combination with optical flow measurements.

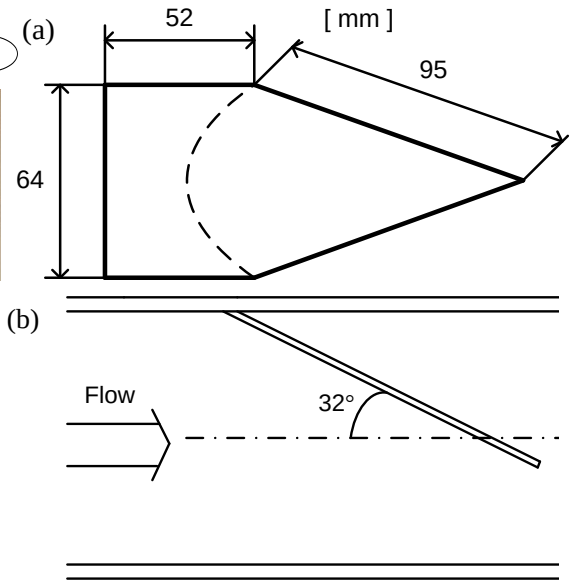

Fig 12. Test object (a triangular plate) used in the experiments a) Vortex mixer plate dimensions b) Vortex mixer angle of attack when mounted

The measurement rig shown in Fig. 2 is connected to the sub-sonic wind tunnel facility at the Marcus Wallenberg Laboratory which provides a silent inlet air flow. The best microphone array for the wave decomposition methods, slightly differs between the methods, while for the source determination it is important to have long microphone distances. In an attempt to satisfy both criteria here, an array with a tight cluster of three equidistant microphones in between two microphones a long distance apart (~1m) is constructed on both sides of the two-port. The axial flow velocity is measured a short distance upstream of the test object pipe using a Prandtl pipe, and the temperature is checked at the outlet of downstream pipe. The mean Mach number based upon an assumed factor (0.82) between the mean and the axial velocity is used when comparing wave decomposition methods. This is motivated by the fact that only one of the methods is able to solve for the real part of the wavenumbers. For the source determination, the solved real part of the wavenumber is used.

The frequency range is limited by the cut-on of the first non-planar mode in the duct, which at Mach 0.2 is approximately 2190 Hz. In order to measure the passive part accurately, a high signal to noise ratio is required. For this reason stepped sine excitation was used. From previous studies of the mixer plate [19], the frequency range containing narrow band variations in the source magnitude was found to be 200 - 500 Hz. For this reason, the stepped sine increments were chosen to be 20 Hz in the ranges 50 - 200 Hz and 500 - 2000 Hz, while in the range 200 - 500 Hz the increments were 5 Hz. Since the number of frequency points is large, the measurement time spent on each point is cut short in order to ensure that the system remains stationary. In this case the number of averages was 64 and the frequency resolution was set to 5 Hz, corresponding to a measurement time of approximately half an hour per loudspeaker setup. The

cross spectra in the source determination measurement were calculated using 8000 averages, corresponding to a measurement time of little less than half an hour.

4. RESULTS AND DISCUSSION

4.1 Effect Of Microphone Holder Configurations

The six different types of holders were tested for flow Mach numbers from M = 0.07 to M = 0.26. The test object was in this case a straight hard-walled pipe. The signal-to-noise ratio was determined by first measuring the noise generated by the loudspeaker at the microphone position without flow. Then the loudspeaker was turned off and the microphone signal was measured again with flow. Random noise was used as input signal and 300 frequency domain averages were made in all cases.

As a first step the holder configurations expected to give similar results were tested against each other. First comparisons were made between holders with similar design such as holder 3 and 4, with a 1,5 mm and 3 mm long cavity respectively. Since the smaller cavity, holder 3 gave a slightly better result it was used for subsequent comparisons. When comparing holder 5, axial slit, and 6, axial slit with a 6.4 mm diameter hole it was found that holder 5 is slightly better for low frequencies while holder 6 is slightly better for high frequencies. It was decided to use holder 5 for subsequent comparisons. Fig. 13 shows the difference in signal-to-noise ratio for holders 2, 3 and 5 compared to the reference holder for M=0.16. The result is similar for other Mach-numbers. A negative S/N ratio in dB means that the results are worse than for the reference holder and a positive S/N ratio that they are better. It was concluded that the reference holder configuration gave the best signal-to-noise ratio. All subsequent tests of signal enhancement techniques were therefore made using this holder.

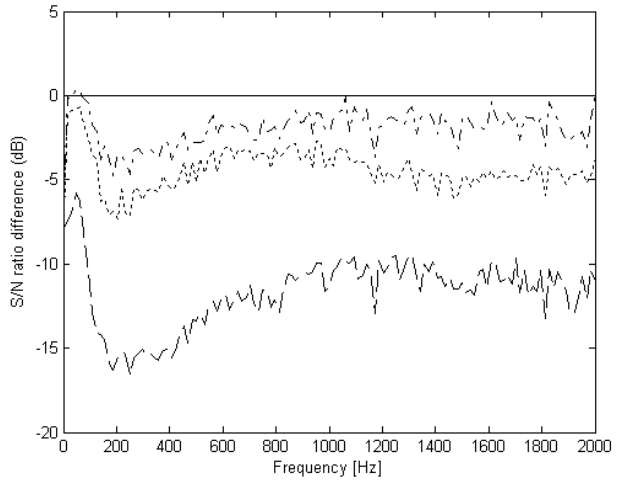

Fig 13. Difference in signal-to-noise ratio compared to the reference holder at M=0.16. —, reference holder; ─ · ─, holder 2; ·····, holder 3; ----, holder 5.

4.2 Effect Of Varying The Loud speaker Connections

The effect of different designs, see Fig. 9, for connecting the loudspeaker to thee duct was tested. For each loudspeaker configuration the signal-to-noise ratio was measured at all six microphone positions. As examples of the results Fig. 14-16 shows the results for M = 0.3 with the source on the downstream side for all three configurations. For the configuration according to Figure 9 a) it can be seen that the flow noise dominates above 500 Hz. As could perhaps be expected this configuration is therefore not so useful. The configuration according to Figure 9 b) reduces the flow noise at the interface between the side-branch and the main pipe but the source level is also reduced leading to an insufficient signal-to-noise ratio. The third configuration according to Figure 9 c) gives the best results as can be seen in Figure 16. This is therefore the loudspeaker mounting configuration used in the remainder of the study.

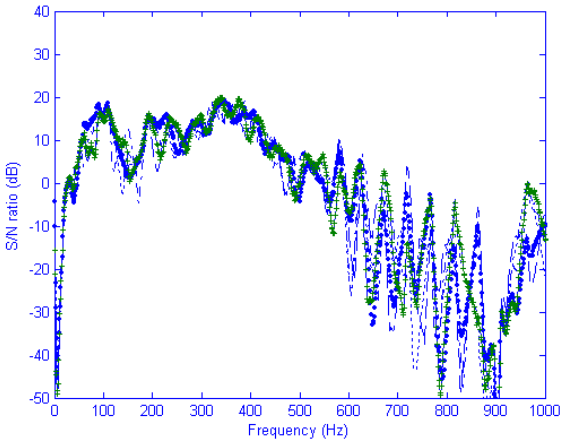

Fig 14. Signal-to-noise ratio at the six microphone positions using the loudspeaker mounting configuration according to Figure 9 a) with the source on the up-stream side using 1000 averages at M=0.3. —, Mic.1; ---, Mic. 2; -.-.-., Mic. 3; ….., Mic. 4; ⋆⋆⋆⋆, Mic. 5; ++++ Mic. 6.

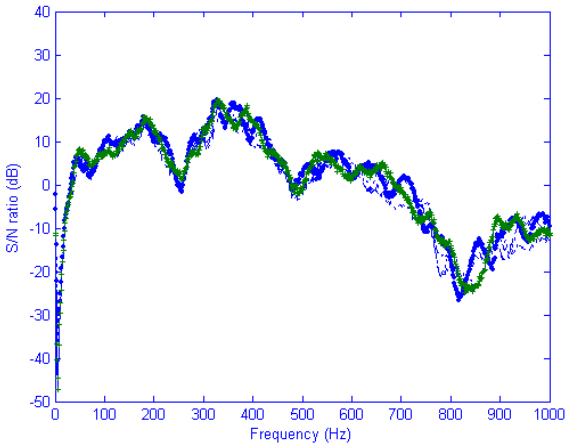

Fig 15. Signal-to-noise ratio at the six microphone positions using the loudspeaker mounting configuration according to Figure 9 b) with the source on the down-stream side using 1000 averages at M=0.3. —, Mic.1; ---, Mic. 2; -.-.-., Mic. 3; ….., Mic. 4; ⋆⋆⋆⋆, Mic. 5; ++++ Mic. 6.

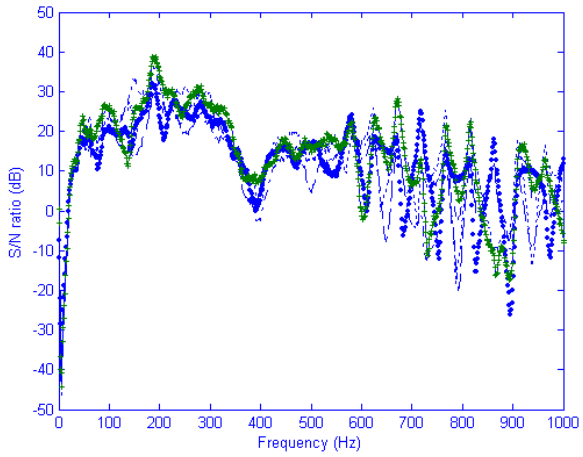

Fig 16. Signal-to-noise ratio at the six microphone positions using the loudspeaker mounting configuration according to Figure 9 c) with the source on the down-stream side using 1000 averages at M=0.3. —, Mic.1; ---, Mic. 2; -.-.-., Mic. 3; ….., Mic. 4; ‘‘‘‘, Mic. 5; ++++ Mic. 6.

4.2 Effect Of Signal Enhancement For Single Microphone Measurement

4.2.1 Frequency domain averaging (FDA)

The test setup previously described was used. The signal-to-noise ratio was determined by first measuring the noise generated by the loudspeaker at the microphone position without flow. Then the loudspeaker was turned off and the microphone signal was measured again with flow. A deterministic signal consisting of a saw-tooth signal with a fundamental frequency of 40 Hz was used. The signal and flow noise measurements were made using standard FFT and auto spectrum estimation procedures. This can be regarded as the reference case since no special signal enhancement techniques have been applied. Measurements were taken for different flow Mach numbers from M = 0.07 to M = 0.21 and with different levels of the output signal exciting the loudspeaker giving 96, 116, 128, 136, and 142 dB sound pressure level at the microphone position.

Fig. 17 shows, as an example of the results, the sound pressure level for the acoustic signal and the flow noise for different numbers of frequency domain averages, for the case with 128 dB sound pressure level and M = 0.21. Since traditional frequency domain averaging only reduces the statistical fluctuations of the flow noise without reducing the level the only effect of the averaging is a smoothing of the flow noise spectrum curves.

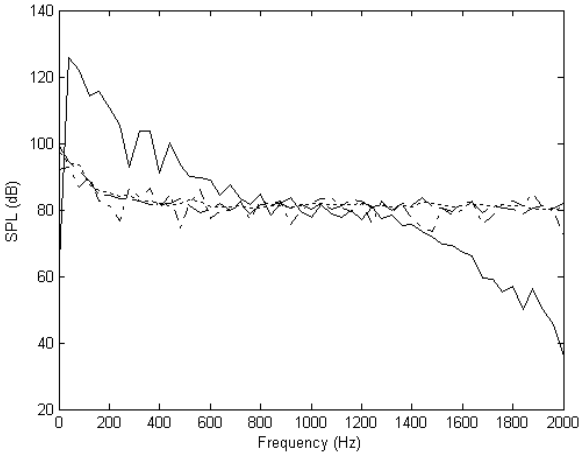

Fig 17. Sound pressure level for the acoustic signal and flow noise using frequency domain averaging, SPL =128dB at M=0.21. —, acoustic signal; flow noise: ─ · ─,1 average; – – –, 10 averages; ·····,100 averages.

4.2.2 Synchronised time domain averaging

The test setup was the same as described in the previous section. The signal-to-noise ratio was also in this case determined by first measuring the noise generated by the loudspeaker at the microphone position without flow. Then the loudspeaker was turned off and the microphone signal was measured again with flow. A deterministic signal with a noise free reference for the synchronisation of the averaging was needed in this case. A saw-tooth signal was used with a fundamental frequency of 40 Hz. Measurements were taken for different flow Mach numbers from M = 0.07 to M = 0.21 and with different sound pressure levels at the microphone position (98, 116, 128, 136, 142 dB).

Fig. 18 shows the sound pressure level for the signal and the flow noise for different numbers of time domain averages, for a 128 dB signal level. The expected decrease in flow noise level by approximately 10 dB when the number of averages is increased by a factor 10 can be observed. It can be seen that the signal dominates over the flow noise up to around 800 Hz for $M = 0.21$ and at the fundamental frequency (40 Hz) there is a S/N-ratio of 30 dB. To study how this technique performs under more adverse conditions the signal level was lowered to 116 dB and 96 giving a 12 and 32 dB decrease in signal level compared to the 128 dB case. For the 116 dB case the signal was still higher than the flow noise up to around 400 Hz and by applying 100 time domain averages it is possible to extract the signal from the flow noise up to around 800 Hz. Further up additional averaging would be required. For the 96 dB case the signal was completely buried in the flow noise from the start but by applying 100 averages it was possible to extract the signal up to around 400-500 Hz.

It can be concluded that applying N number of synchronised time domain averages gives a reduction of the flow noise by a factor $1/N$ or by $10 \cdot Log(N)$ dB.

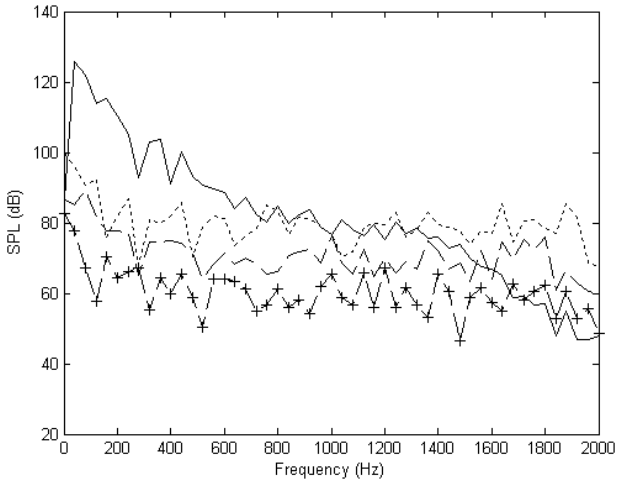

Fig 18. Sound pressure level for the signal and flow noise using time domain averaging, SPL= 128 (dB), M=0.21. —, signal; ·····, 1 average; – – – , 10 averages;— · —, 50 averages;– – +, 100 averages.

4.3.3 Cross-spectrum based frequency domain averaging (CSFDA)

In this case the signal-to-noise ratio was not determined as in the previous sections. Measurements were instead made with both acoustic signal and flow. The same deterministic signal with a noise free reference as for the synchronised time domain averaging, i.e., a saw-tooth signal with a fundamental frequency of 40 Hz was used. The measurements were made using the cross spectrum between the reference signal and the microphone signal and the auto spectrum of the reference signal as described in equation (7). Measurements were also here taken for flow Mach numbers M = 0.07 and M = 0.21 and with different levels of the acoustic signal at the microphone position giving sound pressure levels: 96, 116, 128, 136 and 142 dB. Fig. 19 shows an example of the comparisons of sound pressure level measured using standard frequency domain averaging and calculated using equation 87), i.e., estimated using cross-spectrum based frequency domain averaging. Results for the no flow case are also included in the figure giving an indication of what the signal level should be without the presence of the flow noise. The sound pressure level at the microphone will change slightly when flow is present due to two reasons. The fist is that the sound field in the duct will change due to convective effects of flow and additional turbulent attenuation. There is also a possibility that the sensitivity of the microphone or the sound generation by the loudspeaker may be changed slightly by the presence of the flow, an effect one usually chooses to ignore since it is so difficult to get information about it. The interesting part of the figure is the high frequency part above 1200 Hz where the flow noise starts to dominate the spectrum obtained using standard frequency domain averaging. It can be seen that using cross-spectrum based frequency domain averaging with 100 averages it is possible to extract the signal even when the S/N-ratio originally is as bad as –40 dB. The estimated signal is also reasonably close to the no flow result indicating that the flow effects mentioned above influencing the sound pressure level at the microphone position are small compared to the signal-to-noise ratio increase obtained.

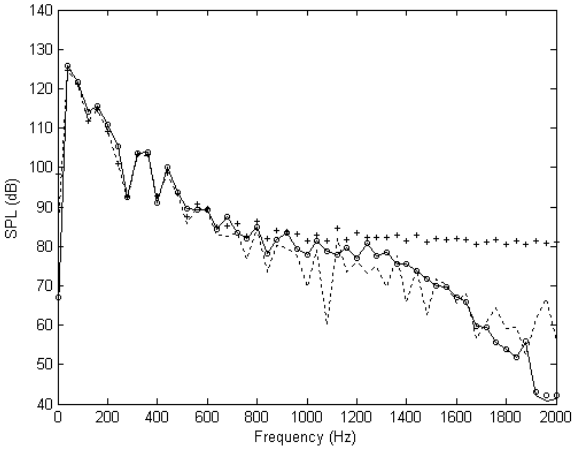

.

Fig 19. Sound pressure level, SPL=128 (dB), M=0.21, 100 averages measured using FDA and CSFDA, for different flow speeds.
○, FDA , —, CSFDA at M=0; ◊, FDA, – – –, CSFDA at M=0.07, +++, FDA, , ·····, CSFDA at M=0.21.

4.3.4 Comparison between synchronised time domain averaging (STDA) and cross-spectrum based frequency domain averaging (CSFDA)

In this section comparisons are made of the result obtained using the tested signal enhancement techniques for measurements on the acoustic signal with flow. Fig. 20 shows the sound pressure level obtained using standard frequency domain averaging, synchronised time domain averaging and cross-spectrum based frequency domain averaging, for a low level acoustic signal and two different flow speeds. It can be seen that applying synchronised time domain averaging and cross-spectrum based frequency domain averaging gives a similar improvement in signal-to-noise ratio compared to ordinary frequency domain averaging.

To make a comparison of the averaging methods used under more controlled conditions some numerical simulations were made. The purpose was to study the outcome of the tested techniques when the same set of input data was used for all three techniques. The experimental results were obtained for the same flow velocities but the results shown in Fig. 20 were not obtained starting from the same set of input data. One purpose of the numerical simulations was therefore to see if the differences between the outcome of synchronised time-domain averaging and cross-spectrum based frequency domain averaging is caused by the different flow noise records used or if the methods in fact give slightly different results. In the first test an impulse train was used as the acoustic signal giving a spectrum with constant level for all frequencies and the frequency was made non-dimensional using the sampling frequency. The acoustic signal level was normalised to give a zero dB reference at all frequencies. The conclusion was that synchronised time domain averaging and cross-spectrum based frequency domain averaging gave exactly identical

results when the same set of input data was used. To show that identical results were obtained also in a measurement situation a test case was set up where the acoustic signal was a saw-tooth signal with a 40 Hz repetition frequency. The input signal and the microphone signal were recorded on DAT-tape for off-line analysis using the different averaging techniques on the same set of data. Time domain averaging and cross-spectrum based frequency domain averaging again gave identical results while a reduction in the flow noise contamination could be seen compared to ordinary frequency domain averaging.

One question, which can also be addressed easily by numerical simulation, is if it makes any difference if the acoustic signal also consists of random noise. Obviously synchronised time domain averaging will not work in this case. Exactly the same result was obtained as when the acoustic signal was periodic. Obviously so called periodic, or pseudo random, noise, that is when the acoustic signal is a random noise signal with the length of one time record used for the averaging which is repeated periodically, would also give the same result. In this case it is however also possible to use synchronised time domain averaging. One of the reasons for changing from random noise excitation to periodic excitation, for instance stepped sine excitation, is that further increasing the number of averages does not seem to give any further improvement. If a reference signal is available so that cross-spectrum based frequency domain averaging can be used it seems from the conclusions above that there should be no difference between the signal-to-noise improvement for different types of excitation signals. The main reason for the improvement when using stepped sine excitation is that the initial signal-to-noise ratio is improved by concentrating the signal energy to one frequency at a time. In theory it should anyway be possible to extract the acoustic signal by averaging, but this may be limited by equipment dynamic range drift or other test set-up stationarity problems for long measurement times. To show that these results could be reproduced in experiments a test case was designed where the acoustic signal was random noise with a level 10 dB below the flow noise level at around 500 Hz. For lower frequencies the difference was smaller while it was larger for higher frequencies. The flow noise level and the level of the acoustic signal obtained using 1000 ordinary frequency domain averages are shown in Figure 18. Fig. 22 shows the sound pressure level for the flow noise contaminated acoustic signal for different number of averages estimated using ordinary frequency domain averaging and cross-spectrum based frequency domain averaging. It can be seen that it is possible to extract the acoustic signal even though it is significantly below flow noise level. At high frequencies we can se the 30 dB reduction in flow noise with 1000 cross-spectrum based frequency domain averages.

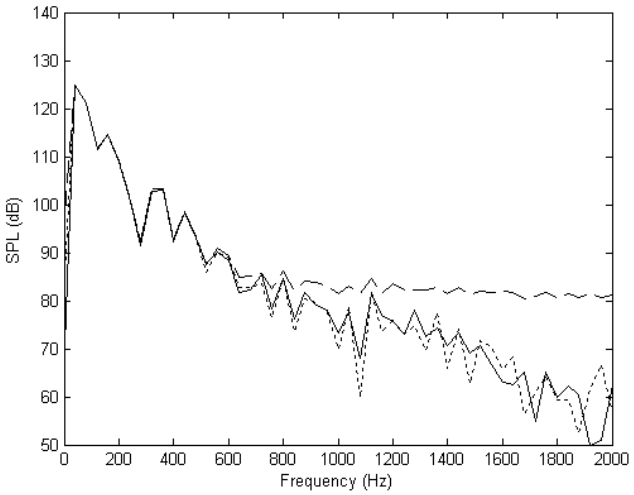

(b).

Fig 20**.** Sound pressure level , SPL= 128 (dB), M=0.21, 100 averages obtained using: —, STDA, – –, FDA, ·····, CSFDA.

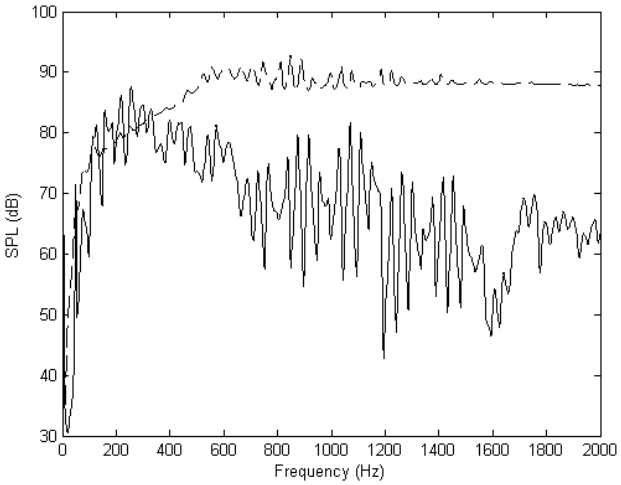

Fig 21**.** Sound pressure level at microphone position obtained using 1000 averages for; —, acoustic excitation only; – – –, flow noise only.

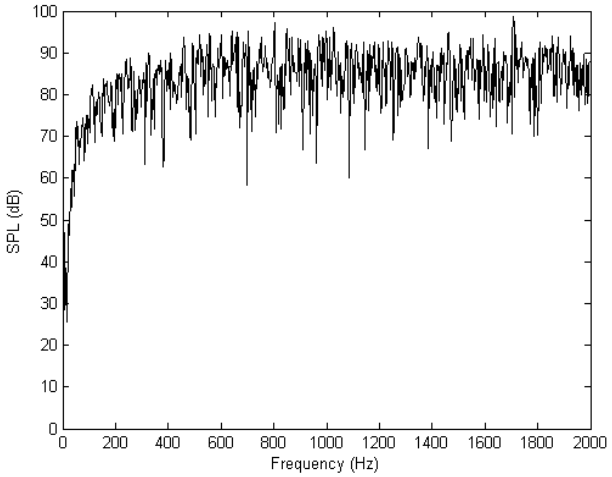

(a) 1 average.

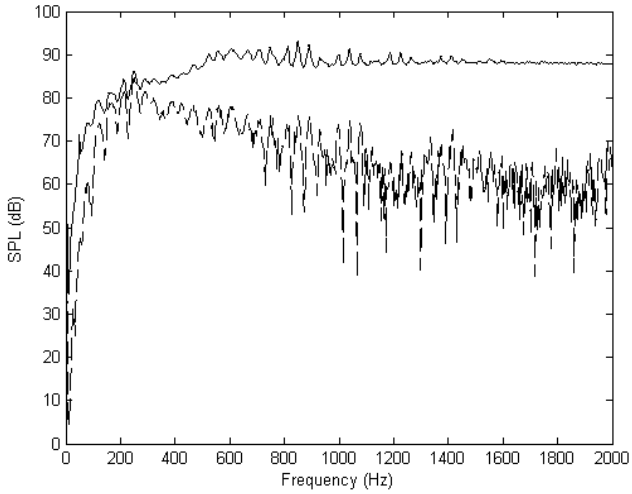

(b) 1000 averages

Fig 22. Sound pressure level for the flow noise contaminated signal estimated using, FDA, — and CSFDA, – – –.

4.3 Effect Of Signal Enhancement For Two-Port Measurement s

4.3.1 Straight duct

The two port data results for the straight duct have been measured and the results compared to theoretical solutions. In the absence of flow Kirchhoff's exact solution has been used and with mean flow results from Dokumaci [65] has been used. For the case without flow the different signal processing techniques give the same result and in agreement with theory. The effect of the mean flow has been investigated at two different Mach number M=0.17 and M=0.24. As an example of the results with flow Fig.23 shows the real part of the first element of the two-port matrix at M=0.24, and it is clear from the result that using random excitation with 10000 averages (CSFDA), and saw tooth excitation with 10000 averages (STDA), gives the same result as stepped sine excitation with 400 averaging (CSFDA) and the theoretical result.

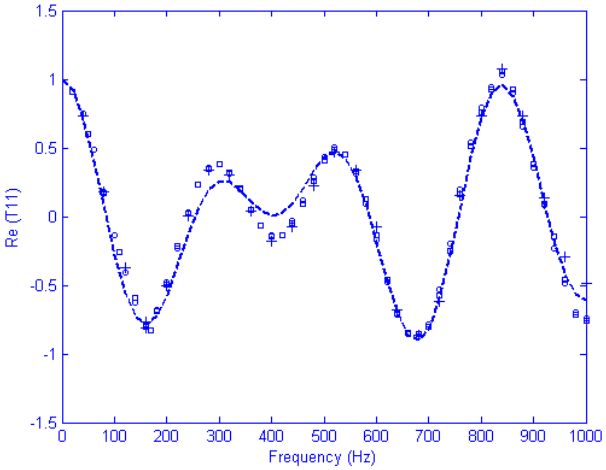

Fig 23. Real part of first element of the acoustic two port for straight pipe at M=0.24 and T=293º K. ---, theory; ↑ ↑ ↑ ↑ , random excitation 10000 averages (CSFDA); oooo, stepped sine excitation 400 averages (CSFDA); ++++, saw tooth excitation 10000 averages (STDA).

4.3.2 Expansion Chamber

Also for the expansion chamber results using stepped sine excitation with 400 cross-spectrum based frequency domain averages (CSFDA) have been used as the reference against which the other results are compared. At M=0.23 using ordinary frequency domain averaging (FDA) did not give good results over the whole frequency range due to poor signal to noise ratio. Increasing the number of averages and using CSFDA gives an improvement in the signal to noise ratio by 10 log (N) dB, where N is the number of averages. Fig. 24 shows a comparison between stepped sine excitation 400 averages (CSFDA), random excitation 10000 averages (CSFDA) and saw-tooth excitation 10000 averages (STDA) for M = 0.3. Since STDA improves the signal to noise ratio by 10 log (N) dB just as CSFDA they give the same result. The results show that excellent results can be obtained at this relatively high flow velocity.

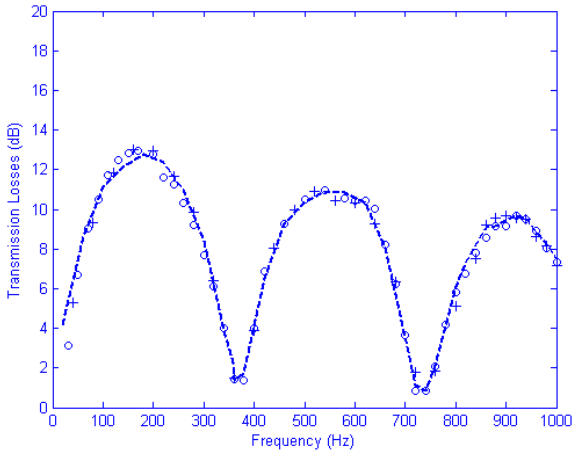

Fig 24. Transmission loss versus frequency for different type of excitations at M=0.3. ----, random excitation with 10000 averages (CSFDA); oooo stepped sine with 400 averages (CSFDA); ++++, saw tooth excitation with 10000 averages (STDA).

If a noise free reference signal is not available an improvement can be obtained by using the microphone with the highest signal to noise ratio as the reference as discussed in section 2. Fig. 25 shows a comparison of the result obtained using microphone 4 as the fixed reference microphone and using the microphone with the highest signal-to-noise ratio for each frequency as the reference. The comparison is made using stepped sine excitation and 400 cross-spectrum based frequency domain averages for M=0.32. It can be seen that at this high flow velocity a slight improvement is obtained when the highest signal-to-noise ratio microphone is used as reference. This technique can therefore give an extra improvement in the most difficult measurement situations.

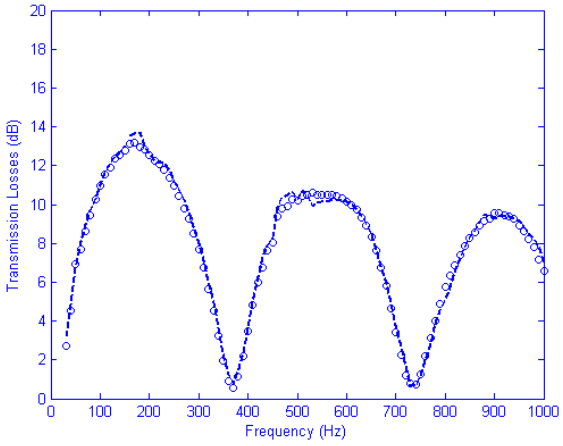

Fig 25. Transmission loss versus frequency for expansion chamber.
Stepped sine excitation with 400 averages (CSFDA) at M=0.325 ----, fixed reference; oooo highest signal-to-noise ratio microphone as reference.

4.3.3 Commercial Muffler

This commercial automotive muffler gives a high transmission loss which makes it a more difficult measurement object compared to the straight duct and the simple expansion chamber studied in the previous sections. Transmission loss has been measured for three different flow velocities (M=0, 0.2, and 0.26). For the no flow case all excitation signals and signal processing techniques gave identical results. Fig. 26 shows results for the ordinary frequency domain averaging (FDA) and cross-spectrum based frequency domain averaging (CSFDA) at M=0.2. The results show that random excitation with FDA gives results which are not in agreement with the reference case, stepped sine excitation and 400 averages, at all frequencies. This is the case even if a very high level input signal is used. CSFDA with 10000 averages gives the same result as the stepped sine excitation. Fig. 27 show results for saw tooth excitation and synchronised time domain averaging (STDA) with 1000 averages and 10000 averages at M = 0.26. For this high flow velocity 1000 averages was not sufficient to give a good result but with 10000 averages a result in agreement with the stepped sine result was obtained.

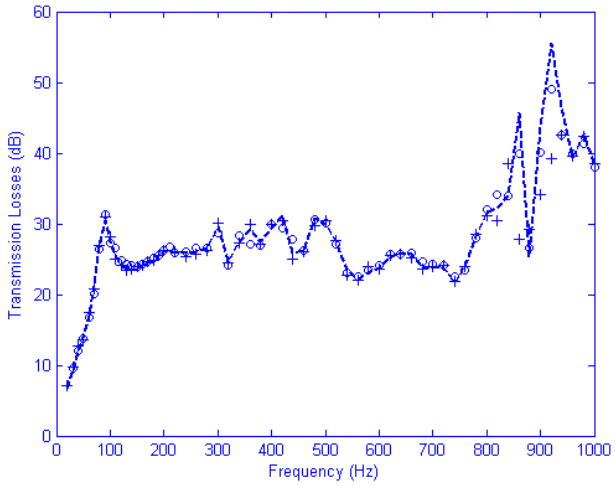

Fig 26. Transmission loss versus frequency for different type of excitations at M=0.2. Random excitation; ---- 10000 averages (CSFDA); +++1000 averages (FDA); oooo stepped sine excitation with 400 averages (CSFDA).

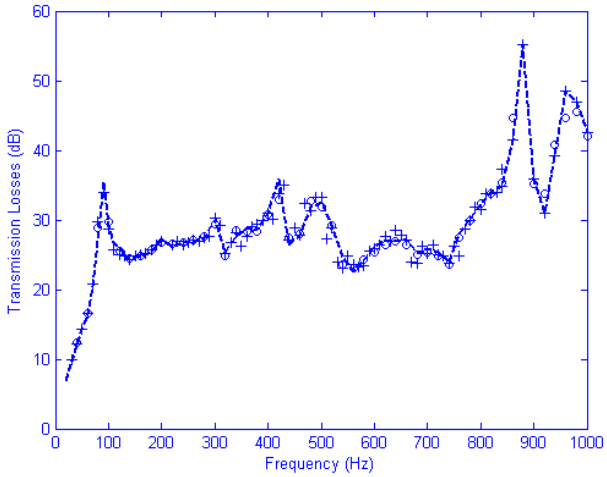

Fig 27. Transmission losses versus frequency for different type of excitations at M=0.26. ----, random excitation with 10000 averages (CSFDA); oooo stepped sine excitation with 400 averages (CSFDA); ++++, saw tooth excitation with 10000 averages (STDA).

4.4 Wave decomposition results

Several measurements of the scattering properties of the straight duct two-port have been conducted by using different loudspeaker combinations. A total of six combinations were created by simply using one loudspeaker at a time, i.e. three measurements with upstream excitation and three with downstream excitation. It was found that the best way to use the redundant measurements was to consider the coherence function between the loudspeaker signal and each microphone, for each measurement and frequency. Thus, out of the three upstream loudspeaker measurements, the two with the lowest coherence, all microphones considered, were rejected. This was repeated for the downstream loudspeaker measurements and at each frequency. The wave decomposition methods were then applied on this synthesized pair of measurements.

Results of the scattering matrix without the plate, obtained using the pressure amplitude over-determination method are shown in Fig. 28 for the magnitude, and in Fig. 29 for the phase. To study the influence of the microphone spacing limits in Eq. (17), results are obtained both with and without taking the limits into consideration. The same comparison for the multi-point method is shown in Fig. 30 for the magnitude and in Fig. 31 for the phase.

The scattering matrix indicates that the presence of the plastic pipe results in transmission loss of the order of 5-30%, for both directions, with some of the energy being reflected. Also, the phase is not zero for any of the transmission elements, which would be the case if the propagation was calculated properly. As will later be shown, the phase error of the transmission elements is mainly due to an incorrect Mach number estimate.

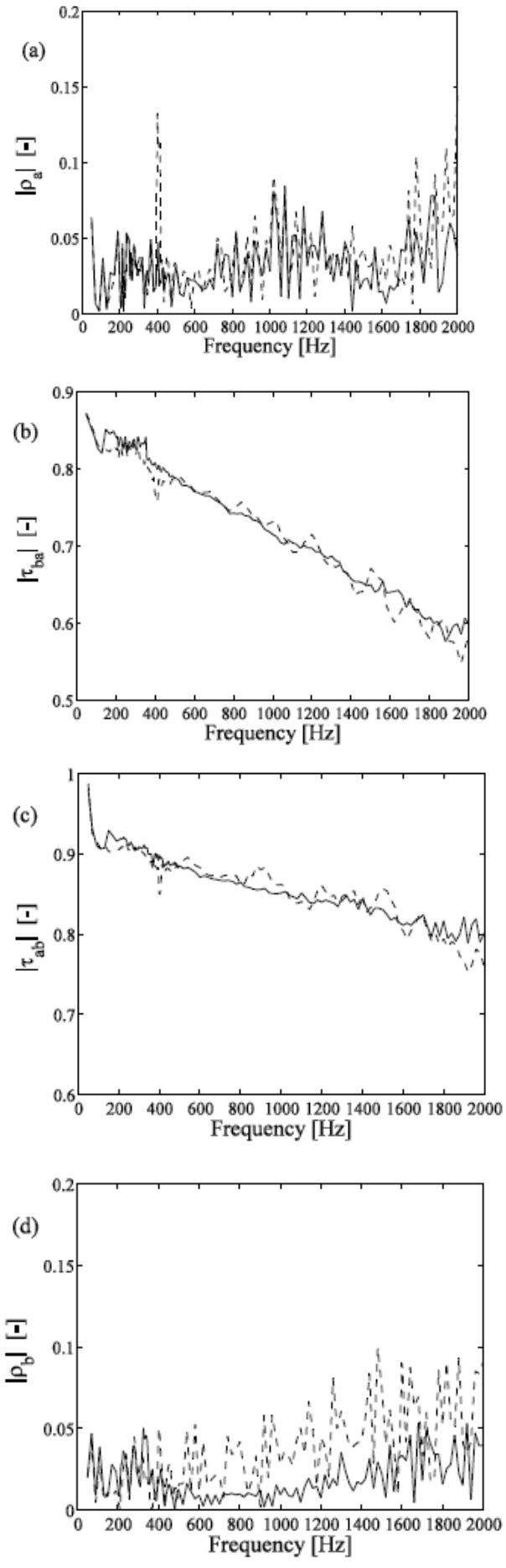

Fig 28. The magnitude of the scattering matrix without the plate, obtained using over-determination; (a), upstream reflection coefficient ρ_a, (b), downstream to upstream transmission coefficient τ_{ab}, (c), upstream to downstream transmission coefficient τ_{ab}, (d), downstream reflection coefficient ρ_b. Solid line: microphones fulfilling Eq. (17) used, dashed line: all microphones used.

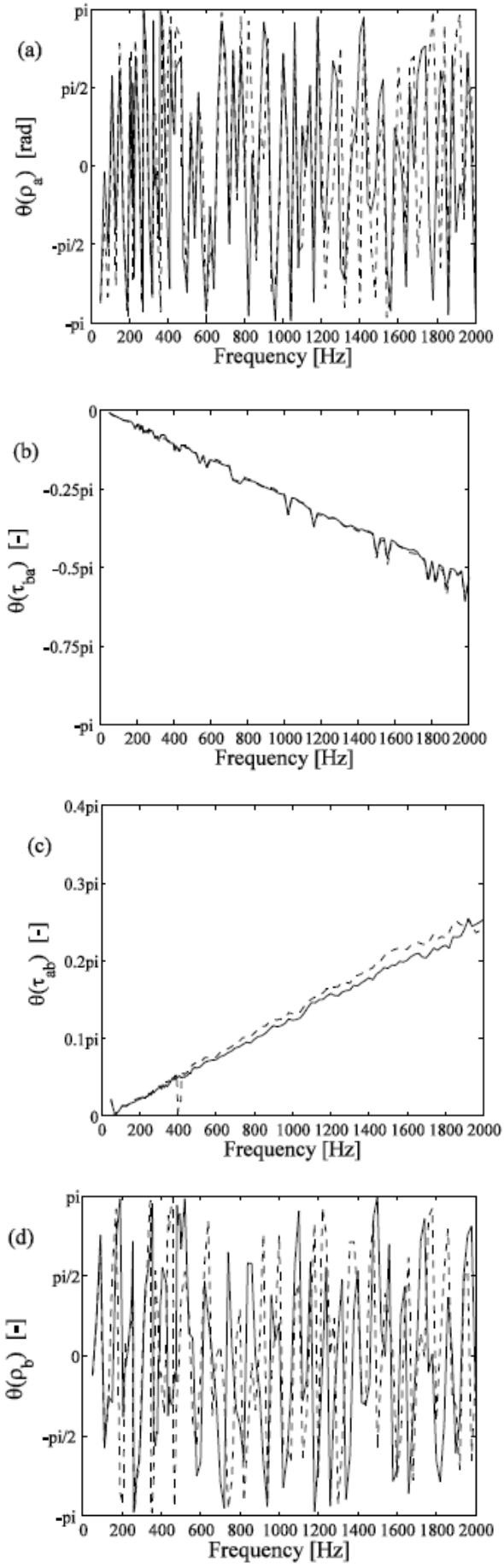

Fig 29. The phase of the scattering matrix without the plate, obtained using over-determination; (a), upstream reflection coefficient ρ_a, (b), downstream to upstream transmission coefficient τ_{ab}, (c), upstream to downstream transmission coefficient τ_{ab}, (d), downstream reflection coefficient ρ_b. Solid line: microphones fulfilling Eq. (17) used, dashed line: all microphones used.

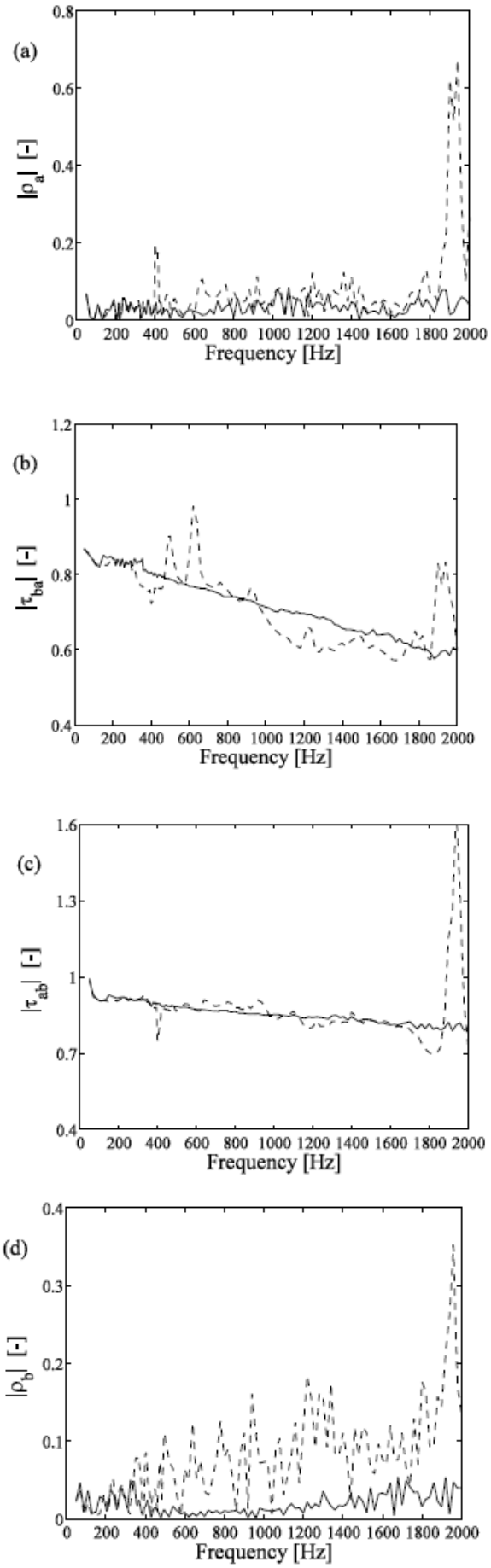

Fig 30. The magnitude of the scattering matrix without the plate, obtained using multi-point method; (a), upstream reflection coefficient ρ_a, (b), downstream to upstream transmission coefficient τ_{ab}, (c), upstream to downstream transmission coefficient τ_{ab}, (d), downstream reflection coefficient ρ_b. Solid line: microphones fulfilling Eq. (17) used, dashed line: all microphones used.

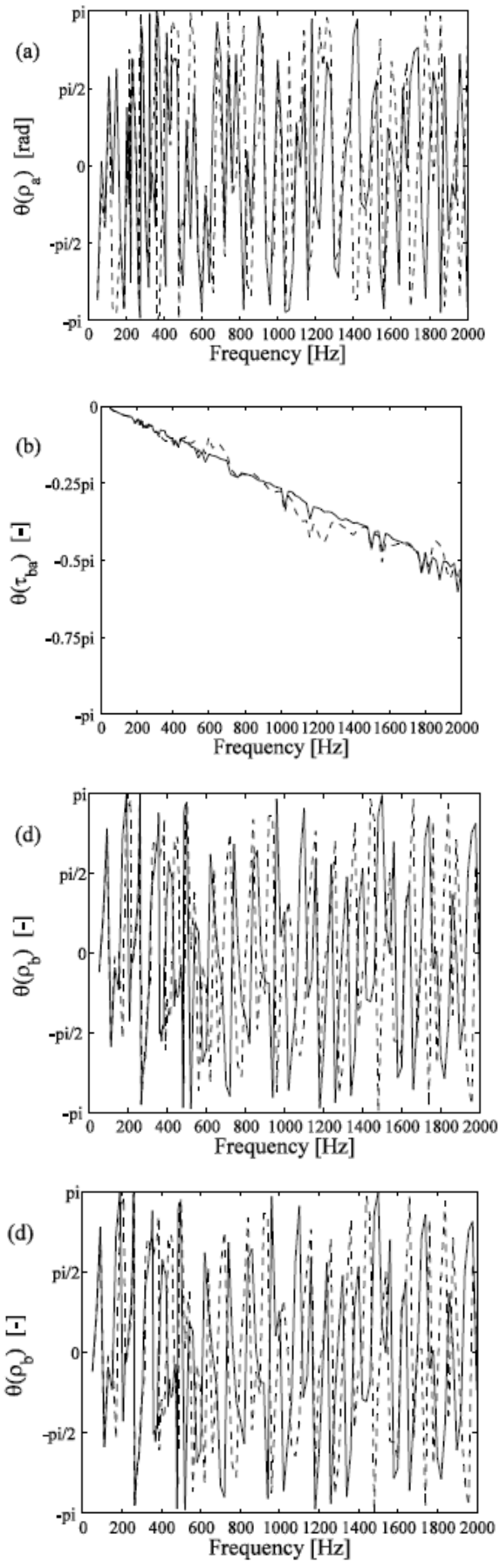

Fig 31**.** The phase of the scattering matrix without the plate, obtained using multi-point method; (a), upstream reflection coefficient ρ_a, (b), downstream to upstream transmission coefficient τ_{ab}, (c), upstream to downstream transmission coefficient τ_{ab}, (d), downstream reflection coefficient ρ_b. Solid line: microphones fulfilling Eq. (17) used, dashed line: all microphones used.

It is seen that the frequency variation become much smoother, both for the over-determined pressure amplitude method and the multi-point method, when the limits in Eq. (17) are considered, despite that the system is still redundant at all frequencies when the limits are disregarded. Also, the multi-point method and the over-determination method yield results which differ less than 1 % from each other when the limits in Eq. (17) are considered.

A third comparison is made between the over-determination method (with the limits in Eq. (17) taken into consideration) and the two-microphone method for which at each frequency, the microphone pair that best satisfied Eq. (18) was applied. The comparison is shown in Fig. 32 for the magnitude and in Fig. 33 for the phase. Although the difference in the results obtained from the two methods is small, there seem to be a magnitude bias error in the frequency range 950 Hz to 1400 Hz in the magnitude of the transmission elements, when the two-microphone method is applied. The origin of the error can be traced to the microphone pair used in that frequency range, suggesting that the bias error is due to either erroneous microphone spacing or calibration factors. Regardless, the over-determination method is superior in this aspect since the larger number of microphones used suppresses the bias error. Since both methods yields similar results in all other frequency ranges these results suggests that the over-determination or the multi-point method should be applied whenever possible.

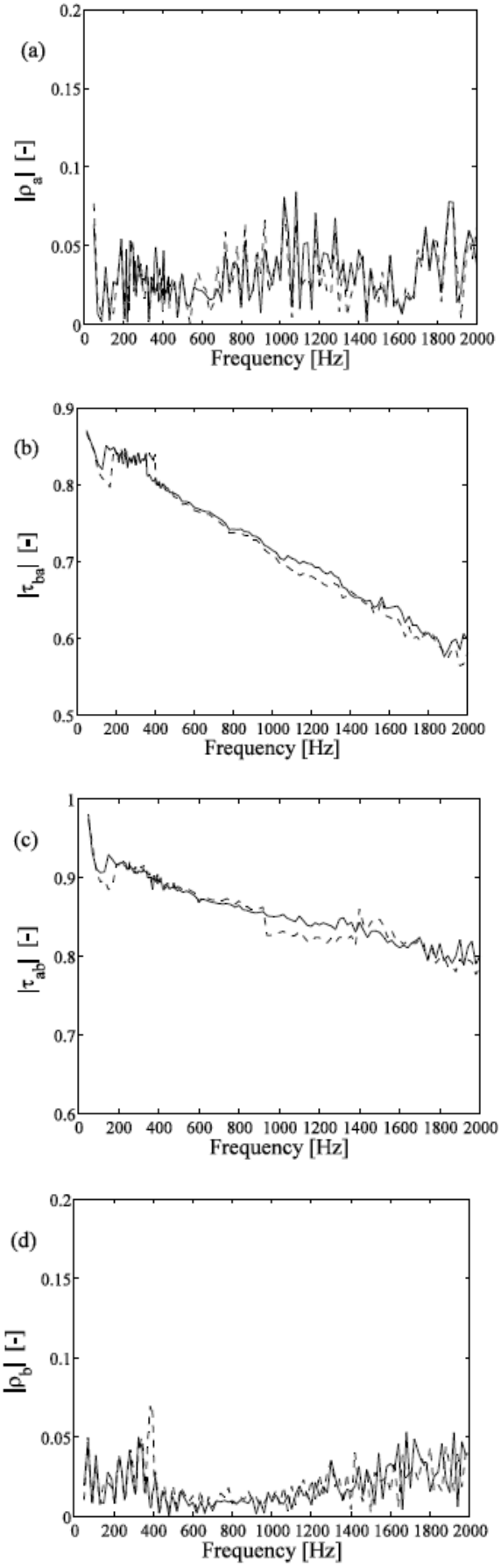

Fig 32**.** The magnitude of the scattering matrix without the plate; (a), upstream reflection coefficient ρ_a, (b), downstream to upstream transmission coefficient τ_{ab}, (c), upstream to downstream transmission coefficient τ_{ab}, (d), downstream reflection coefficient ρ_b. Solid line: obtained using over-determination; with microphones fulfilling Eq. (17) used, dashed line: two-microphone method, where at each frequency, the microphone pair best satisfying Eq. (18) was used.

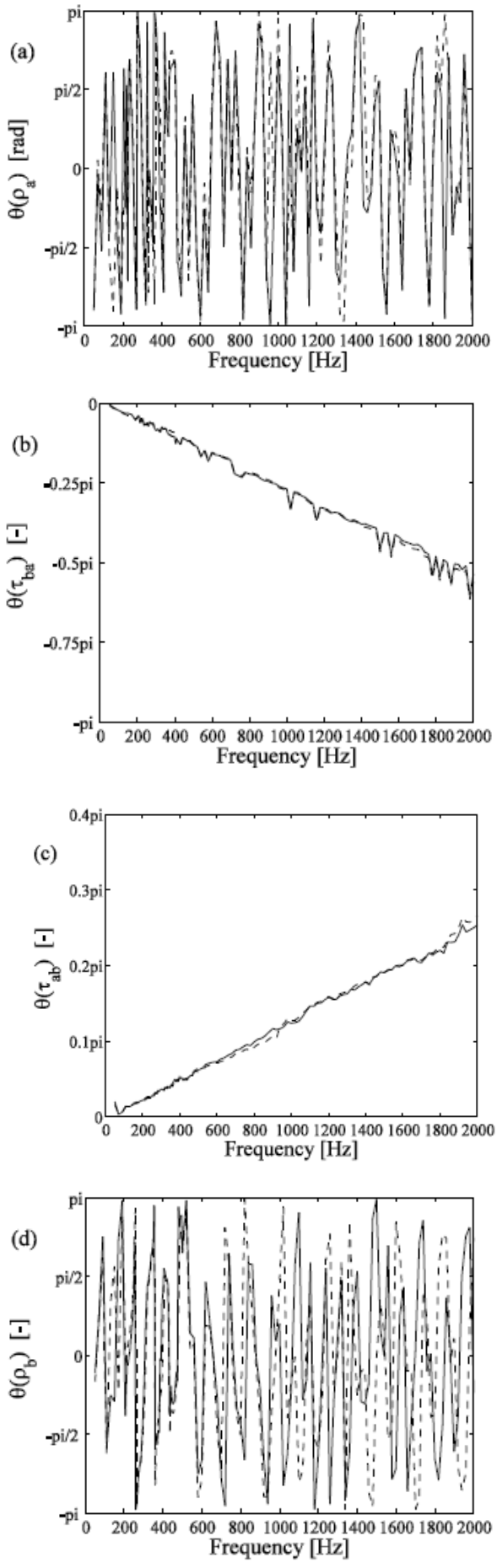

Fig 33. The phase of the scattering matrix without the plate; (a), upstream reflection coefficient ρ_a, (b), downstream to upstream transmission coefficient τ_{ab}, (c), upstream to downstream transmission coefficient τ_{ab}, (d), downstream reflection coefficient ρ_b. Solid line: obtained using over-determination; with microphones fulfilling Eq. (17) used, dashed line: two-microphone method, where at each frequency, the microphone pair best satisfying Eq. (18) was used.

The full wave decomposition method developed by Allam and Åbom [64], was tried for all measurements on the microphone arrays on both sides of the test rig. The conclusion of this is that the method suggested by Allam and Åbom is not applicable using the "short" microphone arrays typical for most in-duct measurements. However, the Mach number determination method introduced in this paper, only require the real part of the waves, and is thus applicable in this case. The results after seven iterations with an initial value of M=0.05 are shown in Table 2.

Table 2: Mean Mach numbers obtained from wavenumbers in the +/- direction via iteration using the full wave decomposition method [5]. Iteration number 0 denotes the initial guess.

Iteration	0	1	2	3	4
$M(k_+)$	0.0500	0.0466	0.2170	0.2072	0.2073
$M(k_-)$	0.0500	0.0466	0.1691	0.2086	0.2079
Iteration	5	6	7		
$M(k_+)$	0.2074	0.2073	0.2074		
$M(k_-)$	0.2078	0.2078	0.2078		

As can be seen, the method converges quickly from a poorly chosen initial Mach number. The mean Mach number obtained from the Prandtl tube in the rig, using 0.82 as the ratio between mean and maximum flow velocity, is 0.201 while the average Mach number calculated from acoustic data is 0.208, i.e. there is a deviation slightly above 3%. In order to analyze the influence of this deviation, the over-determination method using the allowed microphones with respect to the limits in Eq. (17), was applied in the calculation of the scattering matrix, using the model by Dokumaci with each Mach number as input. The magnitude of the scattering matrix is shown in Fig. 34, and the phase is shown in Fig. 35.

It is clear from this result that from an acoustical point of view, the mean Mach number obtained from the wave numbers is more accurate than that obtained from Prandtl tube measurements. It should be kept in mind, that there is relatively large sensitivity to wavenumber errors for such long propagation (2.86 m) calculations. For instance, increasing the temperature from 21 to 22 degrees Celsius in the calculations (but keeping the determined Mach number constant) will change the

phase of element τ_{ab} at 2000 Hz from about 0.14 to -0.04 radians, i.e. to a much more accurate value. However, for the phase of τ_{ba} this temperature change will decrease the phase at the same frequency from -0.19 to -0.47, i.e. increasing the error. This is due to the fact that for a fixed Mach number a temperature change will affect both wavenumbers in the same way, while a Mach number modification (for a fixed temperature) will increase one of the wavenumbers and decrease the other, thus allowing for both the phase of τ_{ab} and of τ_{ba} to approach zero as the Mach number is modified.

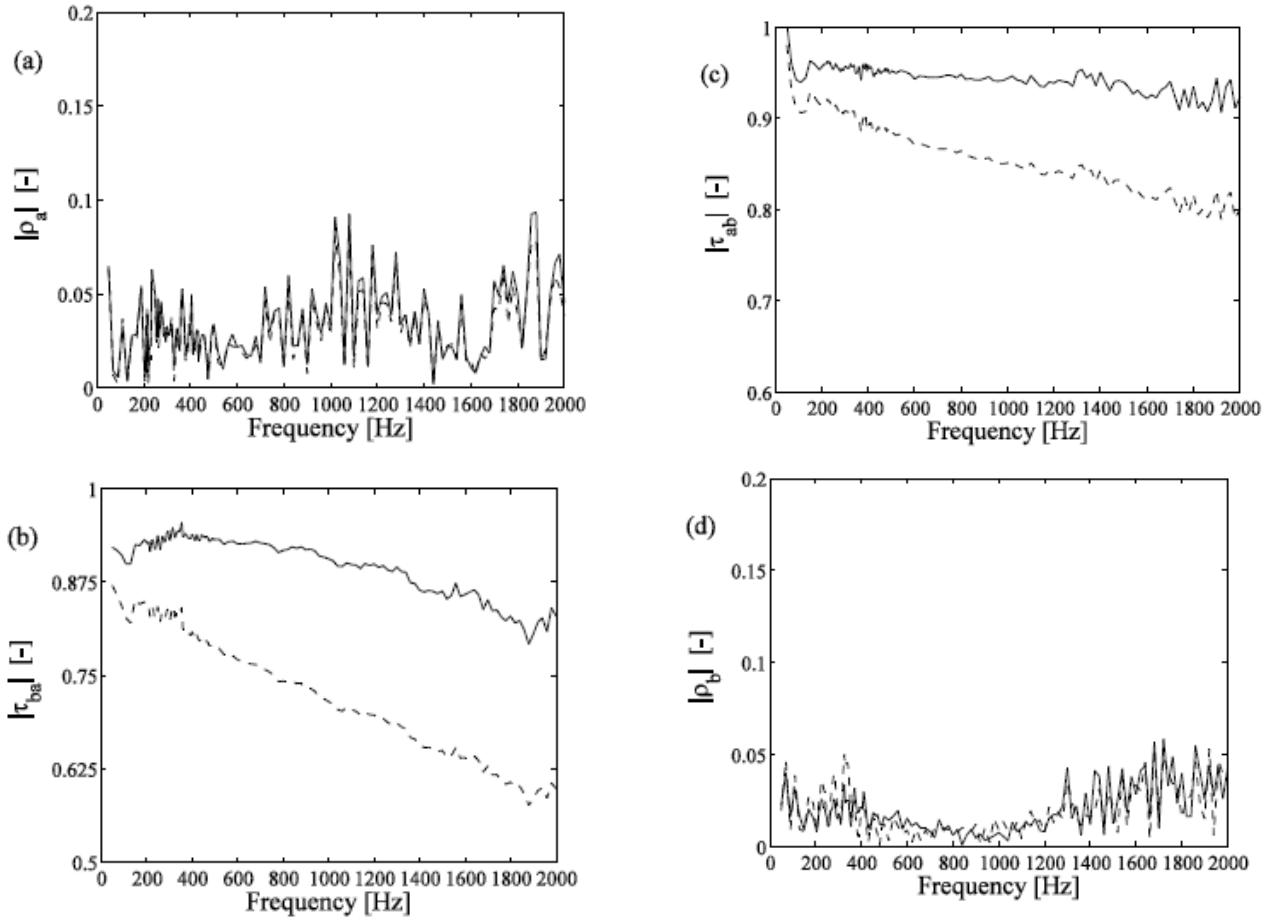

Fig 34.The magnitude of the scattering matrix without the plate, obtained using over-determination, with microphones fulfilling Eq. (17) used; (a), upstream reflection coefficient ρ_a, (b), downstream to upstream transmission coefficient τ_{ab}, (c), upstream to downstream transmission coefficient τ_{ab}, (d), downstream reflection coefficient ρ_b. Solid line: Mach number from acoustic measurements (M = 0.207) used, dashed line: Mach number from Prandtl pipe measurements (M = 0.201) used.

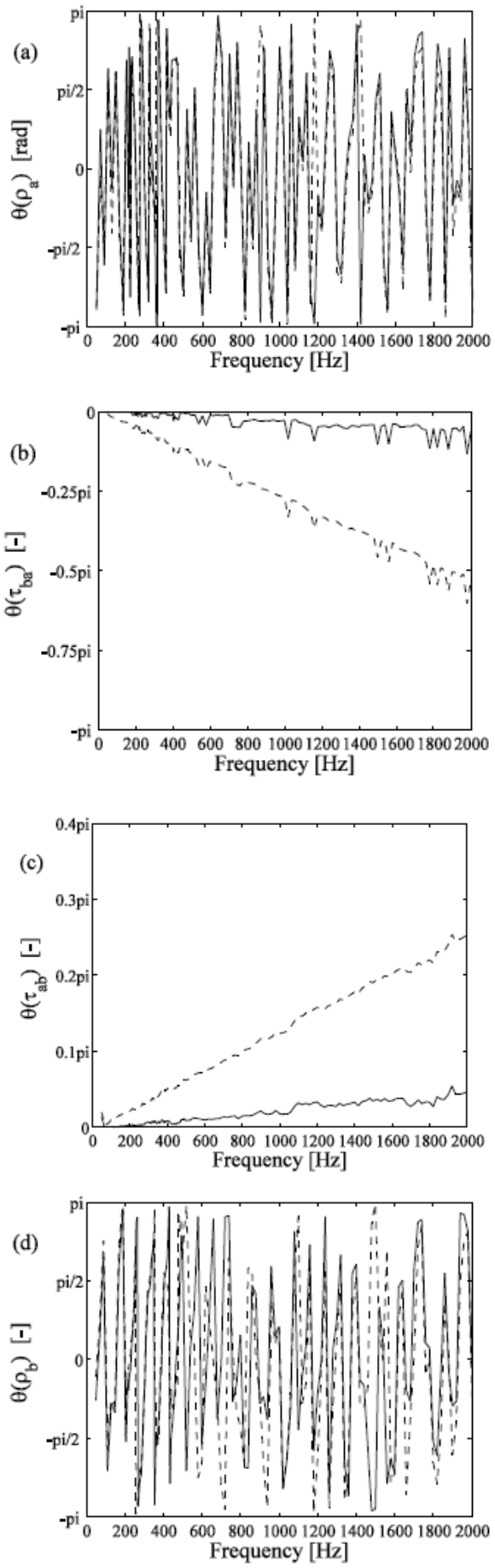

Fig 35. The phase of the scattering matrix without the plate, obtained using over-determination, see section 2.1.2, with microphones fulfilling Eq. (6) used; (a), upstream reflection coefficient ρ_a, (b), downstream to upstream transmission coefficient τ_{ab}, (c), upstream to downstream transmission coefficient τ_{ab}, (d), downstream reflection coefficient ρ_b. Solid line: Mach number from acoustic measurements (M = 0.207) was used, dashed line: Mach number from Prandtl pipe measurements (M = 0.201) was used.

4.5 Scattering And Interaction Results Of The Vortex Mixer Plate

To evaluate the over-determined method for the source part, the cross spectrum matrix is measured with and without the mixer plate. To study the effect of varying the number of microphones in the source measurement, the results are calculated using four different combinations of the available microphones;

A. Microphones 1 and 6 for the first pressure vector in Eq. (43), and 5 and 10 for the second, i.e. the two pairs which will yield the longest intermediate distances, see Fig. 2.
B. Microphones 1, 2, 6 and 7 for the first source vector, and 5 and 10 for the second.
C. Microphones 1 to 4 and 6 to 9 for the first vector, and 5 and 10 for the second.
D. Microphones 1, 2, 3, 6, 7 and 8 for the first vector and 4, 5, 9 and 10 for the second.

All the combinations contain microphones 1 and 5 on the upstream side, and 6 and 10 on the downstream side since they are the furthest apart, thus maximizing the frequency range. Combination A corresponds to the original method by Lavrentjev et al. [18]. Combination B, on the other hand, leads to an over-determination since three microphone pairs are used. C and D both contain all microphones. However, among the two, C yields the lowest frequency at which all microphones are allowed according to the limit in Eq. (33), while D maximizes the number of cross spectra used in the calculations at the frequencies where all microphone distances are sufficiently long. Combination C is, therefore, more suited for the low frequency range, while D should be applied for higher frequencies. An algorithm that switches from C to D at the frequency where D will yield a larger **G** matrix in Eq. (43), could in principle be implemented. However, as will be seen, the choice between C, D and even B, is not crucial for the current test case.

The sound pressure level on each side of the two-port, obtained from the magnitude of the diagonal elements in the source cross spectrum matrix, are shown in Fig. 36, where for the source determination the microphone combination A was used.

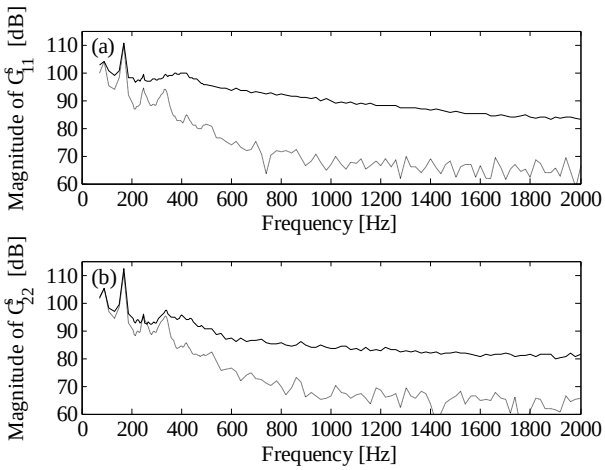

Fig 36. The diagonal elements of the source cross spectrum matrix obtained using the two microphone sets 1, 6 and 5, 10, i.e., no over-determination, (a) magnitude of G^s_{11}, (b) magnitude of G^s_{22}, "-----" empty duct, "——" mixer plate.

The point of going through with a full two-port determination, is that once obtained, the scattering matrix and the source cross spectrum matrix can be used to calculate the sound field in any duct system the two-port element is to be mounted in. Thus to validate a determined two-port, a straight-forward way is to put the two-port element in another test rig, where the sound field is firstly calculated and then measured for validation. Of course, it is even faster and cheaper to just modify the downstream end termination. The latter is applied in this paper.

To validate the determined source cross spectrum matrix, the auto and cross spectra for all microphones are measured after the downstream end termination is modified by removing the muffler and ventilation hose. By measuring the reflection of this new end termination and using the source cross spectrum matrix already determined, these cross and auto spectra can in theory be obtained by reformulating Eq. (32)

$$\begin{bmatrix} G_{p_a p'_a} & G_{p'_b p_a} \\ G_{p'_a p_b} & G_{p_b p'_b} \end{bmatrix} = \mathbf{C}^{-1}\mathbf{G}^s\left(\mathbf{C}'^{\dagger}\right)^{-1} \qquad (49)$$

However, as effort has been made to suppress the influence of flow noise on the results, the cross spectra and in particular the auto spectra obtained using Eq. (34) will be less noise contaminated than the measured ones. This does limit the robustness of this validation procedure; in general a good agreement between calculated and measured result means that the two-port is accurately determined, but large deviations does not necessarily mean the opposite. However, as will be shown, it is a minor problem at most frequencies in this application. The validation is presented in Figs. 37 and 38, where the calculated cross spectra have been obtained from the source cross spectrum matrix determined using microphones 1-3 and 6-8 for the first vector and 4, 5, 9 and 10 for the second.

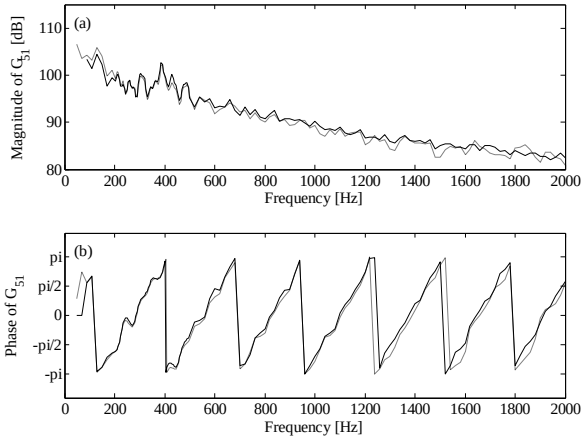

Fig 37. The cross spectra G_{51}, (a) magnitude, (b) phase, obtained via "-----" measurement, "——" calculations from G^s obtained using microphones 1-3, 6-8 and 4, 5, 9, 10.

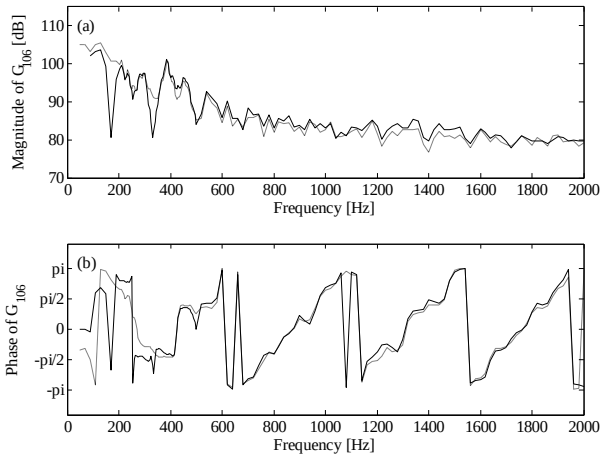

Fig 38. The cross spectra G_{106}, (a) magnitude, (b) phase, obtained via "-----" measurement, "——" calculations from G^s obtained using microphones 1-3, 6-8 and 4, 5, 9, 10.

For the cross spectrum obtained from upstream microphones (Fig. 36) there is a good agreement for both the magnitude and the phase. However, for the cross spectrum obtained from the downstream microphones (Fig, 37) some large discrepancies can be found at discrete frequencies in the low frequency range. This is most likely due to an increased flow noise generation at the downstream duct termination, which is not suppressed by 8000 averages of the cross spectra. In other words, the cross spectrum measured contain contributions from both the two-port source and from external sources. Overall, however, the agreement between the predicted and the measured cross spectra is satisfactory. It should be noted here that one requirement for the validation to work is that the air flow in the test rig remains unmodified when the end termination is changed. The reason for this is that the two-port is a function of the

in- and outlet flow conditions. Thus, the source data will not be valid for other flow conditions, which could occur if, for instance, the static pressure drop is significantly modified when the muffler is removed. In the present case though, the velocity was not observed to be influenced noticeable by this.

5. SUMMARY AND CONCLUSIONS

Measurement of acoustic signals, with application to two-port data measurements in flow ducts, in the presence of masking noise generated by mean flow has been studied in this paper. Different techniques to increase signal-to-noise ratio have been investigated. A number of different microphone holder configurations were studied and it was concluded that the reference microphone holder with a flush mounted transducer gave the best result. A number of possible configurations for connecting the loudspeakers needed to excite the flow duct element under test have been investigated. It was concluded that using a perforate pipe section with about 50% porosity between the loudspeaker side branch and the duct was the beast out of the studied configurations. Two different signal enhancement techniques were tested: synchronised time domain averaging and cross-spectrum based frequency domain averaging. They were compared to the result of ordinary frequency domain averaging as found in any FFT analyser. The conclusion was that synchronised time domain averaging and cross-spectrum based frequency domain averaging gave equally good results. Both gave a signal-to-noise ratio improvement of N or $10 \cdot Log(N)$ dB, where N is the number of averages. It was also found that when using cross-spectrum based frequency domain averaging it does not make any difference for the signal-to-noise ratio improvement if a periodic or a random acoustic signal were used, as long as a noise free reference signal is available. The improvement obtained when shifting from random noise excitation to for instance stepped sine excitation is due to the increase in initial signal-to-noise ratio caused by the concentration of signal energy to one frequency at a time. Two-port data measurements and transmission loss measurements have been made for three different test objects: a straight pipe a simple expansion chamber and a commercial automotive muffler with high transmission loss. Tests were made for Mach numbers up to 0.3. Different signal processing techniques were tested for reducing the adverse effects of flow noise at the microphones. The most successful techniques require a reference signal which can be either the electric signal being input to the loudspeakers or one of the microphone signals. As a reference technique stepped sine excitation with cross-spectrum based frequency domain averaging was used. This technique could give good results for most cases as far as could be seen. For the straight duct case comparisons with theoretical results were also made. Good agreement was obtained between the experimental and theoretical results. It was shown that using a periodic signal (saw-tooth) and synchronized time domain averaging good results could be obtained if a sufficient number of averages were used. At flow velocities higher than M=0.2 about 10000 averages were needed. Random excitation together with cross-spectrum based frequency domain averaging also gave good result if the same number of averages was used. Ordinary frequency domain averaging was not sufficient at high flow velocities. It was also shown that using the cross-spectrum based frequency domain averaging an improvement could be obtained if the microphone with the highest signal-to-noise ratio at each frequency was used rather than a fixed microphone reference.

In this paper, methods for improving the accuracy of experimental two-port characterization of flow generated sound have been evaluated. Experiments were conducted in a test rig of circular ducts, carrying a mean flow of approximately Mach 0.2, in which a triangular plate was inserted at an angle. For the determination of the scattering matrix and test rig end reflections, several plane wave decomposition methods were tested, which all utilize an abundant number of microphones, i.e. more than two on each side. The best methods were found to be the multi-point method and the over-determination method. It was also found that all intermediate distances between the microphones must fulfill the limits for the two-microphone method in Eq. (6). The results were improved further when the real part of the wavenumbers were determined from the acoustic measurements, improvements which for higher frequencies and long ducts are significant. Using the most accurate method found, the end terminations and the scattering matrix were calculated. From the scattering matrix, a power balance was calculated showing that no significant interaction between the hydrodynamic and acoustic field occurs in the current setup.

For the source, a new over-determination approach of the source cross spectrum matrix was presented. By comparing with the previous method, it was found that applying the over-determination improved the results significantly in the frequency range where the background noise and the two-port source were of similar strength. It is thus concluded that the over-determination technique is an important tool.

6. REFERENCES

1. W. Neise 1975 *Journal of Sound and Vibration* **39**, 371-400. Theoretical and Experimental Investigations of Microphone Probes for Sound Measurements in Turbulent Flow.
2. K. P. Holland and P. O. A. L. Davies 2000 *Journal of Sound and Vibration* **230**, 915-932. The Measurement of Sound Power Flux in the Flow Duct.
3. P.D. Welch 1967, *IEEE Trans. Audio Electroacoust.,* **AU-15**, 70-73. The use of FFT for the estimation of power spectra: A method Based on Time Averaging Over Short Modified Periodograms.
4. M.S. Bartlett 1953, *Cambridge University Press, Cambridge*. An Introduction to Stochastic Processes with Special Reference to Methods and Applications.
5. J.S. Bendat and A. Piersol 1980 *New York: John Wiley& Sons, Inc.*.Engineering Applications of Correlation and Spectral Analysis

6. J.S. Bendat, 1978, *Journal of Sound and Vibration*, **59**, 405-yyy. Statistical Errors in Measurement of Coherence Functions and Input/Output Quantities.
7. T,Y. Lung and A.G. Doige, 1983, *Journal of the Acoustical Society of America*, **73**, 867-876. A Time-Averaging Transient Testing Method for acoustic properties of piping systems and mufflers with flow.
8. R. Sing and T. Katra, 1978, *Journal of Sound and Vibration*, **56**, 279-298. Development of An Impulse Technique for Measurement of Muffler Characteristics.
9. H. Hudde and U. Letens, 1984, *Acustica*, **56**, 258-269. Untersuchungen Zum Akustschen Messleitungsverfahren mit Festem Messorten.
10. S. Braun 1975 *Acustica* **32**, 69-77. The Extraction of Periodic Waveforms by Time domain Averaging.
11. S. Braun and B. Seth 1980 *Journal of Sound and Vibration* **70**, 513-526. Analysis of repetitive mechanism signature.
12. P.D. McFadden 1987 *Mechanical Systems and Signal Processing* **1**, 83-95. A Revised Model for the Extraction of Periodic Waveforms by Time Domain Averaging.
13. P.D. McFadden 1989 *Mechanical Systems and Signal Processing* **3**, 87-97. Interpolation Techniques for Time Domain Averaging of Gear Vibration.
14. L. Hongxing, Z. Hongfu, J. Chengyu and Q. Liangsheng 2000 *Mechanical Systems and Signal Processing* **14**, 279-285. An Improved Algorithm for Direct Time-domain Averaging.
15. B. S. Perlman and V. H. Auerbach 1977 *IEEE Tranactions on Acoustics, Speech, and Signal Processing.*, **4**, 295-299. A Phase-Locking Technique for Estimating the Ensemble Average of Time-Series Data.
16. M. G. Jones 1998 *NASA/TM-1998-208426*. A Comparison of Signal Enhancement Methods for Extracting Total Acoustic Signals.
17. P.R. Wagstaff and J.C. Henrio, 1984, *Journal of Sound and Vibration*, **94**, 156-159. The Measurement of Acoustic Intensity by Selective Two Microphone Techniques with A Dual Channel Analyzer.
18. J. Lavrentjev, M. Åbom and H. Bodén, 1995 *Journal of Sound and Vibration* **183,** 517-531. A Measurement Method for Determining the Source Data of Acoustic Two-Port Sources.
19. J.Y. Chung and D.A. Blaser, 1980, *Journal of the Acoustical Society of America*, **68**, 907-913. Transfer Function Method of Measuring In-duct Acoustic Properties.
20. J.Y. Chung, 1977, *Journal of the Acoustical Society of America*, **62**, 388-395. Rejection of Flow Noise using A coherence Function Method.
21. C.-G. Johansson, M. Mimer and M. Åbom 1998 *Proceedings of InterNoise 98*. Turbulence Suppressing Probes for In-duct Measurements.
22. R.S. McGuinn 1996 *PhD Thesis Pennsylvania State University*.
23. H. P. Wallin and M. Åbom 1986 *Proceeding of the Nordic Acoustic Meeting, 389-391*. Description of A Flow Noise Facility.
24. ISO**10534**-1:1996, Acoustics–Determination of Sound Absorbing Coefficient and Impedance in Impedance Tubes, Part I: Method Using Standing Wave Ratio.
25. ISO **10534**-2:1998, Acoustics–Determination of Sound Absorption coefficient and Impedance method in Impedance Tubes, Part II: Transfer –Function method.
26. V. B. Panicker and M.L. Munjal 1981 *Journal of Sound and Vibration* **77**(4), 573-577 " Impedance Tube Technology for flow Acoustics.
27. A.F. Seybert and D.F Ross 1977 *Journal of Acoustical society of America* **61**, 1362-1370. Experimental Determination of Acoustic Properties Using a Two-microphone Random Excitation Technique.
28. J. Y. Chung and D. A. Blaser. 1980 *Journal of Acoustical society of America* **68**, 907–913 Transfer Function Method of Measuring In-Duct Acoustic Properties I. Theory.
29. J.Y. Chung and D.A. Blaser 1980 *Journal of Acoustical society of America* **68,** 914-921. Transfer Function Method of Measuring In-duct Acoustic Properties, II: Experiment.
30. A.F. Seybert 1988 *Journal of Acoustical society of America* **83,** 2233-2239. Two-sensor Methods for the Measurement of Sound Intensity and Acoustic Properties in Ducts.
31. ASTM standard, **E1050-*98***, 1998. Standard Test Method for Impedance and Absorption of Acoustical Material Using A Tube, Two Microphones and a Digital Frequency Analysis System.
32. W. T. Chu 1991 *Noise control Engineering journal* **37**, 37-41. Impedance Tube Measurements- Comparative Study of Current practices.
33. W. T. Chu 1988 *Journal of Acoustical society of America* **83**, 2225-2260. Further Experimental Studies on the Transfer Function Technique for the Impedance Tube Measurements.
34. H. Bodén and M. Åbom 1986 *Journal of Acoustical society of America* **79** (2), 541-549. Influence of Errors on the Two Microphone Method for Measuring Acoustic Properties in Ducts.
35. M. Åbom and H. Bodén 1988 *Journal of Acoustical society of America* **83,** 2429-2438. Error Analysis of Two-Microphone Measurements in Duct with Flow

36. F. Seybert and B. Soenarko 1981 *Journal of Acoustical Society of America*. **69**, 1190–1199. Error Analysis of Spectral Estimates with Application to the Measurement of Acoustic Parameters Using Random Sound Fields in Ducts.
37. C.W.S. To and A.G. Doige 1979 *Journal of Sound and Vibration* **62**, 207-222. A Transient Testing Technique for The Determination of Matrix Parameters of Acoustic Systems, 1: Theory and Principles.
38. C.W.S. To, and A.G. Doige 1979 *Journal of Sound and Vibration*, ***62***, 223-233. A Transient Testing Technique for the Determination of Matrix Parameters of Acoustic Systems, 2: Experimental Procedures and Results.
39. T.Y. Lung and A.G. Doige 1983 *Journal of Acoustical Society of America* **73**, 867-876. A Time-averaging Transient Testing Method for Acoustic Properties of Piping Systems and Mufflers.
40. M. Nishimura, S. Fukatsu and K. Akamatsu 1983 *Proceeding of Inter-noise* **83**, 395-398. Measurement of Transfer Function Mmatrices of Duct Elements and Source Impedances, Using the Pair-Microphone Technique.
41. F. Payri, J.M. Desantes and A. Broatch, 2000 *Journal of Acoustical Society of America* **107**, 731-738. Modified Impulse Method for the Measurement of the Frequency Response of Acoustic Filters to Weakly Nonlinear Transient Excitations.
42. A.C. Fumoux, D. Leducq and K. Akamatsu 1985 *Proceeding of Inter-noise* **85**, 1239-1242. Transfer-Function Measurement of Hydraulic Piping System Elements.
43. A.G. Doige and M.L. Munjal. 1988 *Proceeding of Noise control* **88**, 481-485. An Improved Experimental Method for Determining Transfer Matrices or Pipe Line Elements with Flow.
44. M.L. Munjal, and A.G. Doige 1990 *Journal of Sound and Vibration* **141**(2), 323-333. Theory of a Two Source-location Method for Direct Experimental Evaluation of the Four-Pole Parameters of an Aeroacoustic Element.
45. M Åbom 1991 *Journal of Mech. System and Signal Proceeding* **5** (2), 89-104. Measurement of the Scattering-Matrix of Acoustical Two-Ports.
46. H. Bodén and M. Åbom 1995. Modelling of fluid machines as sources of sound in duct and pipe systems, *Acta Acustica* **3**, 549-560.
47. H. Bodén 1995. On multi-load methods for determining the source data of acoustic one-port sources, *Journal of Sound and Vibration* **180**(5), 725-743.
48. S. H. Jang and J. G. Ih 2000. Refined multiload method for measuring acoustical source characteristics of an intake or exhaust system, *Journal of the Acoustical Society of America* **107**(6), 3217-3225.
49. M. L. Munjal and A. G. Doige 1990. Theory of a two source-location method for direct experimental evaluation of the four-pole parameters of an aeroacoustic element. *Journal of Sound and Vibration* **141**(2), 323-333.
50. M. Terao and H. Sekine 1989. In-duct pressure measurement to determine sound generation, characteristic reflection and transmission factors of an air moving device in air-flow, *InterNoise 89*, , pp. 143-146.
51. J. Lavrentjev, M. Åbom and H. Bodén 1995. A measurement method for determining the source data of acoustic two-port sources. *Journal of Sound and Vibration* **183**(3), 517-531.
52. M. Åbom, S. Allam and S. Boij 2006, "Aero-acoustics of flow duct singularities at Low Mach-numbers", 12th AIAA/CEAS Aeroacoustics conf., Boston, AIAA, 2006-2687.
53. W. De Roeck and W. Desmet 2008. Experimental acoustic identification of flow noise sources in expansion chambers, *Proceedings of ISMA*, 455-470.
54. M. Karlsson and M. Åbom 2010. Aeroacoustics of T-junctions–An experimental investigation, *Journal of Sound and Vibration* **329**(10), 1793-1808.
55. M. Åbom (1992) *Journal of Sound and Vibration*, **155** (1), 185-1883. A note on the Experimental Determination of Acoustical Two-Port Matrices.
56. A. D. Pierce 1981. *Acoustics: An Introduction to its Physical Principles and Applications*, Mcgraw-Hill, New York.
57. M. L. Munjal 1987. *Acoustics of Ducts and Mufflers*, Wiley-Interscience, New York.
58. P. O. A. L. Davies 1988. Practical flow duct acoustics. *Journal of Sound and Vibration* 124, 91-115.
59. M. Åbom 1991. Measurement of the scattering-matrix of acoustical two-ports. *Mechanical Systems and Signal Processing* **5**(2), 89-104.
60. W. E. Schmidt and J. P. Johnston 1975. Measurement of Acoustic Reflection from Obstructions in a Pipe with Flow. *NSF Report* PD-20.
61. T. Fujimori, S. Sato and H. Miura 1984. An automated measurement system of complex sound pressure reflection coefficients, *InterNoise* 84, 1009-1014.
62. M. G. Jones and T. L. Parrott 1989. Evaluation of a multi-point method for determining acoustic impedance. *Mechanical Systems and Signal Processing* **3**(1), 15-35.
63. G. Dahlquist and Å. Björck 1974. *Numerical Methods*, Prentice Hall Inc, New Jersey.
64. S. Allam and M. Åbom 2006. Investigation of damping and radiation using full plane wave decomposition in ducts. *Journal of Sound and Vibration* **292**, 519-534.

65. E. Dokumaci 1997 *Journal of Sound and Vibration* **208**(4), 653-655 A note on Transmission of Sound in a Wide Pipe with Mean Flow and Viscothermal attenuation.
66. H. Schlichting 1968. *Boundary-Layer Theory*, McGraw-Hill, USA.
67. J. E. Potzick and B. Robertson 1984. Long wavelength acoustic flowmeter, U. S. Patent 4,445,489.
68. W. S. Cheung, H. Kwon, K. A. Park and J. S. Paik 2001. Acoustic flowmeter for the measurement of the mean flow velocity in pipes. *Journal of the Acoustical Society of America* **110**(5), 2308-2314.
69. Y. B. Kim and Y. H. Kim 2002. A measurement method of the flow rate in a pipe using a microphone array. *Journal of the Acoustical Society of America* **112**(3), 856-865.
70. S. Allam, H. Bodén and M. Åbom 2006. Over-determination in acoustic two-port data measurement, *The Thirteenth International Congress on Sound and Vibration*, Vienna, July.
71. Y. Aurégan and R. Starobinski 1999. Determination of acoustical dissipation/production potentiality from the acoustical transfer function of a multiport, *Acta Acustica* **85**, 788-892.
72. M. Karlsson and M. Åbom 2011. On the use of linear acoustic multiports to predict whistling in confined flows, *Acta Acustica united with Acoustica* **97,** 24-33.
73. A. Kierkegaard and G. Efraimsson 201. Simulations of Duct Whistling with Nyquist Analysis and Linearized Navier-Stokes equations, *17th AIAA/CEAS Aeroacoustic Conference*, Portland, June.
74. M. Karlsson, A. Holmberg, M. Åbom, B. Fallenius and J. Fransson 2008. Experimental determination of the aero-acoustic properties of an in-duct flexible plate, *14th AIAA/CEAS Aeroacoustics Conference*, Vancouver, May.

7.MAILING ADDRESS

Hans Bodén
KTH Linné Flow Centre, The Marcus Wallenberg Laboratory, SE-100 44 Stockholm, Sweden